

557.09773
IL6cr 1979-1
✓. 1

**ENGINEERING STUDY OF STRUCTURAL GEOLOGIC FEATURES
OF THE HERRIN (NO. 6) COAL AND ASSOCIATED ROCK IN ILLINOIS**

Volume 1—Summary report

Prepared for

**UNITED STATES DEPARTMENT OF THE INTERIOR
BUREAU OF MINES**

by

**Illinois Institute of Natural Resources,
ILLINOIS STATE GEOLOGICAL SURVEY DIVISION, Urbana, Illinois**

**with contributions by
UNIVERSITY OF ILLINOIS AT URBANA-CHAMPAIGN,
Urbana, Illinois**

FINAL REPORT

**Contract No. H0242017
Engineering Study of Structural Geologic Features
of the Herrin (No. 6) Coal and Associated Rock in Illinois**

June 1979

50272-101

| | | | | | |
|--|--|--|----|--|--|
| REPORT DOCUMENTATION PAGE | | 1. REPORT NO. | 2. | 3. Recipient's Accession No. | |
| 4. Title and Subtitle Engineering Study of Structural Geologic Features of the Herrin (No. 6) Coal and Associated Rock in Illinois. Volume 1—Summary report | | | | 5. Report Date June 1979 (submitted) | |
| 7. Author(s) H.-F. Krausse, H. H. Damberger, (cont. in box 15) | | | | 6. | |
| 9. Performing Organization Name and Address Illinois State Geological Survey, Urbana, IL 61801 with contributions by the University of Illinois at Urbana-Champaign, Urbana, IL 61801 | | | | 8. Performing Organization Rept. No. | |
| 12. Sponsoring Organization Name and Address U.S. Department of the Interior Bureau of Mines Washington, DC | | | | 10. Project/Task/Work Unit No. | |
| 15. Supplementary Notes W. J. Nelson, S. R. Hunt, C. T. Ledvina, C. G. Treworgy, and W. A. White, with contributions by V. D. Brandow, H. M. Karara, and A. S. Nieto (University of Illinois) | | | | 11. Contract(C) or Grant(G) No. (C) H0242017 (G) | |
| 16. Abstract (Limit: 200 words) Roof failures in underground coal mines are related to the lithology and geologic structure of the roof. There are two distinct suites of roof rock above the Herrin (No. 6) Coal in Illinois, and each has distinctive patterns of structure and roof failure. In black shale-limestone roof areas, roof instability is correlated with thinning of limestone beds and presence of faults and clay dikes. In gray shale roof regions, the prime roof hazards are posed by rolls, shear bodies, and presence of coal or carbonaceous partings in the roof. Most structural features examined are believed to have formed during early stages of sediment diagenesis and compaction. Structural trends and lithologic patterns are strongly inter- dependent for this reason. In many cases geologic patterns are so complex and locally variable that prediction of roof stability far in advance of mining is difficult. The need for greater flexibility in roof control planning is apparent. | | | | 13. Type of Report & Period Covered Final | |
| 17. Document Analysis a. Descriptors | | | | 14. | |
| b. Identifiers/Open Ended Terms | | | | | |
| c. COSATI Field/Group | | | | | |
| 18. Availability Statement Release unlimited | | 19. Security Class (This Report) Unclassified | | 21. No. of Pages 54 | |
| | | 20. Security Class (This Page) Unclassified | | 22. Price | |

(See ANSI-Z39.18)

See Instructions on Reverse

OPTIONAL FORM 272 (4-77)
(Formerly NTIS-35)
Department of Commerce

FOREWORD

This report was prepared by the Illinois State Geological Survey in Urbana, Illinois, under USBM contract number H0242017. The contract was administered by the ground control program under the technical direction of the Denver office with Mr. Douglas Bolstad acting as technical project officer. Mr. David Askin was the contract administrator for the Bureau of Mines. The contract extended from March 1974 through February 1976, but results from work beyond that date are also included. This report was submitted by the authors on February 6, 1978, and was resubmitted after revisions in June 1979.

We wish to extend special thanks to the numerous coal company officials and employees who assisted our work by opening their mines to our study, acted as guides, and provided great amounts of valuable information. We want to acknowledge the many Survey staff members, not listed as authors, who contributed to the work, in particular: M. E. Hopkins, who initiated the roof study, Harold J. Gluskoter, William H. Smith, Lawrence E. Bengal, Roger B. Nance, and George J. Allgaier. The core testing was carried out by Mr. Caner Zanback under the supervision of Dr. Lester S. Fruth, both of the Department of Geology at the University of Illinois, Urbana. Without the help of these, and many others, this report would not have been possible.

CONTENTS

Volume 1

| | |
|---|----|
| INTRODUCTION | 1 |
| The geologic setting of the Illinois Basin Coal Field | 1 |
| Techniques employed | 6 |
| ROOF TYPES OF THE HERRIN (NO. 6) COAL MEMBER IN ILLINOIS | 8 |
| Gray shale roof types | 9 |
| Black shale-limestone roof types | 21 |
| MAPS AND EXPLANATION OF THE GEOLOGY IN SELECTED STUDY AREAS | 31 |
| OBSERVATIONS AND DISCUSSION OF ROOF FAILURE TRENDS | 40 |
| MATERIAL PROPERTIES AND DESIGN CRITERIA | 40 |
| CONCLUSIONS | 41 |
| Geologic interpretations | 41 |
| Recommendations | 44 |
| APPENDIX | 47 |
| REFERENCES | 54 |

Figures

| | |
|---|----|
| 1. Stratigraphic section of the Carbondale Formation | 2 |
| 2. Geologic structures of Illinois | 3 |
| 3. Distribution of the Herrin (No. 6) Coal in Illinois | 4 |
| 4. Schematic section of the interval between the Herrin (No. 6) Coal and the Piasa Limestone Member | 5 |
| 5. Map showing area covered by computer mapping | 7 |
| 6. Photograph of roof fall in planar-bedded sandstone of the Energy Shale Member | 11 |
| 7. Sketch of typical roll | 11 |
| 8. Photograph of a roll of medium-gray shale | 12 |
| 9. Photograph of a large siltstone-filled roll | 12 |
| 10. Photograph of a roll in planar-bedded sandstone and siltstone | 13 |
| 11. Detail of figure 10 | 13 |
| 12. Detail of figure 11 | 13 |
| 13. Geologic map of study area 4 | 14 |
| 14. Map of rolls and roof lithologies in study area 5 | 15 |
| 15. Map of shear body, roof lithologies, and roof falls in study area 5 | 16 |
| 16. Geologic map of study area 7 | 17 |
| 17. Photograph of lower boundary of shear body in study area 5 | 18 |
| 18. Detail of figure 17 | 18 |

| | | |
|-----|---|----|
| 19. | Photograph of roll truncated by shear planes in study area 5 | 19 |
| 20. | Photograph of microfaulted shale and siltstone in shear body, study area 5 | 20 |
| 21. | Detail of figure 20 | 20 |
| 22. | Diagram of black shale-limestone roof sequence at mine A | 21 |
| 23. | Map of roof lithologies in study area 1 | 23 |
| 24. | Map of roof lithologies in study area 2 | 24 |
| 25. | Map of roof lithologies in study area 3 | 25 |
| 26. | Photograph of Brereton Limestone roof | 26 |
| 27. | Photograph of wedging relationship of rock layers in black shale-limestone roof | 26 |
| 28. | Photograph of horizons in Lawson Shale | 28 |
| 29. | Photograph of syneresis cracks in the Lawson Shale | 28 |
| 30. | Photograph of clay dike and clay-dike fault | 29 |
| 31. | Detail of figure 30 | 29 |
| 32. | Photograph of complex clay dike in the Herrin (No. 6) Coal | 30 |
| 33. | Diagram of clay-dike faults | 30 |
| 34. | Diagram of clay-dike faults forming a graben | 30 |
| 35. | Map of structural features in study area 1 | 32 |
| 36. | Map of structural features in study area 2 | 33 |
| 37. | Map of structural features in study area 3 | 34 |
| 38. | Computer-generated map of the top of the Herrin (No. 6) Coal in study areas 6 and 7 | 35 |
| 39. | Map of the thickness of the Anna Shale Member in Bond and Montgomery Counties | 36 |
| 40. | Map of the thickness of the Brereton Limestone Member in Bond and Montgomery Counties | 36 |
| 41. | Photograph of a major clay-dike fault showing false drag | 37 |
| 42. | Map of roof lithologies and roof falls in study area 6 | 39 |
| 43. | Diagram of rock strength of roof-pillar-floor materials | 40 |
| 44. | Schematic of the relationship of roof lithology to coal topography | 42 |
| 45. | Interpretative sequence of roll formation | 43 |
| A. | Map of lithology and structural features in study area 1 | 48 |
| B. | Map of lithology and structural features in study area 2 | 50 |
| C. | Map of lithology and structural features in study area 3 | 52 |

Volume 2 (Detailed Report)

| | |
|---|----|
| INTRODUCTION | 1 |
| Statement of goals | 1 |
| Previous work | 2 |
| Selection of study areas and activity plan | 2 |
| THE GEOLOGY OF THE ILLINOIS BASIN COAL FIELD | 3 |
| Characteristics of the coal-bearing strata | 3 |
| Structure of the Herrin (No. 6) Coal Member in the Illinois Basin | 5 |
| Geology of the Herrin (No. 6) Coal Member and its roof strata | 5 |
| The Herrin (No. 6) Coal Member | 7 |
| Geology of the roof strata of the Herrin (No. 6) Coal Member | 7 |
| TECHNIQUES EMPLOYED | 15 |
| Regional mapping using rock-stratigraphic data and computer graphics | 15 |
| Regional maps | 15 |
| Structural maps of mine areas | 17 |
| Detailed geologic mapping of selected study areas in underground mines | 17 |
| Close-range photogrammetry | 18 |
| Object space control and acquisitions of photography | 18 |
| Mensuration and data reduction | 18 |
| Core drilling in underground mines | 19 |
| Core testing | 19 |
| Techniques employed in clay mineralogy studies of various roof and floor rocks | 20 |
| Mechanical, chemical, and optical analyses | 20 |
| Radiography and x-ray diffraction analyses | 21 |
| ROOF TYPES OF THE HERRIN (NO. 6) COAL MEMBER IN ILLINOIS | 23 |
| Gray shale roof types | 23 |
| Lithology and facies of the gray shale roof types | 23 |
| Structures and deformational features of the gray shale roof types | 34 |
| Black shale-limestone roof types | 60 |
| Description of lithology and facies of the black shale- limestone roof types | 60 |

| | |
|---|-----|
| Structures and deformational features in black shale-limestone roof areas | 79 |
| MAPS AND EXPLANATIONS OF THE GEOLOGY IN SELECTED STUDY AREAS | 102 |
| Results of in-mine mapping of selected study areas | 102 |
| Study areas in black shale-limestone roof | 102 |
| Study areas in gray shale roof | 150 |
| Results from computer-generated maps of thickness and structure | 165 |
| OBSERVATIONS AND DISCUSSION OF ROOF FAILURE TRENDS | 173 |
| General observations | 173 |
| Frequency and distribution of roof falls | 175 |
| Fall distribution related to the type of lithology in the immediate roof | 175 |
| Fall distribution related to the occurrence of structural features | 177 |
| Summary of roof fall occurrences | 178 |
| Long-term incidence of instability | 178 |
| MATERIAL PROPERTIES AND DESIGN CRITERIA | 180 |
| Geotechnical data from the literature | 181 |
| Uniaxial compression and deformation modules testing programs | 184 |
| Petrographic factors in shale roof quality | 186 |
| CONCLUSIONS | 191 |
| Geologic significance of the results | 191 |
| Lithology and its distribution | 191 |
| Structures—types and distribution | 193 |
| Effects of the geologic setting on mining | 195 |
| Mine operations on a day-to-day basis | 195 |
| Premining investigation and mine planning | 196 |
| Recommendations | 199 |
| To the mining industry | 199 |
| To the scientific researcher or consultant | 199 |
| BIBLIOGRAPHY | 200 |

Tables

| | |
|---|-----|
| 1. Summary of work progress | 3 |
| 2. Details of mapping for computer-generated maps of thickness and structure | 165 |
| 3. Percentage of intersections of entries and crosscuts with different roof lithologies | 175 |
| 4. Percentage of intersections of entries and crosscuts with different structural features in the roof strata | 175 |
| 5. Relation of stable and fallen intersections and roof falls | 176 |
| 6. Occurrence of fallen intersections for different roof lithologies | 176 |
| 7. Occurrence of fallen intersections for different structural features | 177 |
| 8. Lithology and structural distribution as a percentage of fallen intersections by study area | 178 |
| 9. Roof fall distribution coefficients | 179 |
| 10. Uniaxial compression and E-modulus, test results | 185 |
| 11. Clay mineralogy analyses of various rock types in the Illinois Basin Coal Field | 187 |
| 12. Orientation and content of clay minerals at sample height above the Herrin (No. 6) Coal in Christian County, Illinois | 189 |
| 13. Comparative thickness of Anna Shale and Brereton Limestone | 193 |

Figures

| | |
|--|----|
| 1. Stratigraphic section of the Carbondale Formation | 4 |
| 2. Arrangement of lithologic units in a cyclothem | 4 |
| 3. Geologic structures of Illinois | 6 |
| 4. Distribution of the Herrin (No. 6) Coal in Illinois | 8 |
| 5. Thickness of the Herrin (No. 6) Coal in Illinois | 9 |
| 6. Schematic section of the interval between the Herrin (No. 6) Coal and the Piasa Limestone Members | 9 |
| 7. Lithologic sections of the gray shale roof type | 11 |
| 8. Lithologic sections of the black shale-limestone roof type | 13 |
| 9. Map showing area covered by computer mapping | 16 |
| 10. Sample data entry form | 16 |
| 11. Classification chart for siliceous clastic rock types | 20 |
| 12. Photograph of dark-gray shale eroded by drilling fluid | 20 |
| 13. Calculation form for mineral contents in argillaceous sediments | 22 |
| 14. Diffractograms of a well-laminated shale | 22 |
| 15. Diffractograms of a claystone | 22 |
| 16. Photograph of top coal left by boring type of continuous miner | 25 |
| 17. Photograph of top coal left by ripper type of continuous miner | 25 |
| 18. Rose diagram of orientation of tree trunk imprints | 27 |
| 19. Photograph of roof fall in planar-bedded siltstone in the Energy Shale Member | 31 |
| 20. Photograph of roof fall in planar-bedded sandstone of the Energy Shale Member | 31 |
| 21. Photograph of roof fall in Anvil Rock Sandstone Member | 32 |
| 22. Photograph of wedge in the Energy Shale Member | 33 |
| 23. Diagram of a small lens of Energy Shale | 33 |
| 24. Photograph of planar-bedded sandstone and bedding-plane anomalies | 35 |

| | |
|--|----|
| 25. Isopach map of shale in split coal | 37 |
| 26. Photograph of concretions in gray shale roof | 38 |
| 27. Photograph of small synsedimentary slump and load structures | 38 |
| 28. Photograph of explosion structure in coal | 39 |
| 29. Sketch of typical roll | 40 |
| 30. Sketch of small fold in the Herrin (No. 6) Coal Member | 41 |
| 31. Diagram of soft-sediment folds in a roll | 41 |
| 32. Photograph of a specimen of a small roll | 41 |
| 33. Photograph of a roll of medium-gray shale in coal | 42 |
| 34. Diagram of gray shale rolls | 42 |
| 35. Diagram of gray shale roll | 43 |
| 36. Diagram of a complex gray-shale roll | 44 |
| 37. Photograph of large siltstone-filled roll | 44 |
| 38. Photograph of a roll in planar-bedded sandstone and siltstone | 45 |
| 39. Detail of figure 38 | 45 |
| 40. Detail of figure 39 | 45 |
| 41. Photograph of small pod of medium-gray shale | 46 |
| 42. Photograph of small-scale high-angle faults | 48 |
| 43. Photograph of gray shale roll sheared into several blocks | 49 |
| 44. Photograph of small clay dike under gray shale roof | 49 |
| 45. Diagram of roof failure caused by low-angle shear surfaces | 50 |
| 46. Photograph of shear plane parallel to bedding | 51 |
| 47. Photograph of microfaulted finely laminated silty shale between low-angle shears | 51 |
| 48. Photograph of lower boundary of shear body, study area 5 | 52 |
| 49. Detail of figure 48 | 52 |
| 50. Photograph of roof fall in shear body of mine B | 53 |
| 51. Photograph of roof fall in shear body of mine B | 53 |
| 52. Photograph of roll truncated by shear planes in study area 5 | 54 |
| 53. Photograph of microfaulted shale and siltstone in shear body, study area 5 | 54 |
| 54. Detail of figure 53 | 55 |
| 55. Diagram of microfaulted laminated silty shale and siltstone | 55 |
| 56. Schmidt net density diagrams of shear planes | 56 |
| 57. Photograph of narrowly spaced parallel joints in dark-gray shale | 57 |
| 58. Diagram of roof fall development | 58 |
| 59. Map of major fault systems and structures in southern Illinois | 59 |
| 60. Diagram of black shale-limestone roof sequence at mine A | 61 |
| 61. Photograph of "bastard limestone" | 62 |
| 62. Diagram of lens of "bastard limestone" | 62 |
| 63. Photograph of strip-mine highwall showing black shale-limestone roof sequence | 63 |
| 64. Stratigraphic cross sections prepared from photogrammetry | 64 |
| 65. Photograph of subunits of the Anna Shale Member | 65 |
| 66. Photographs of Anna Shale and Brereton Limestone | 65 |
| 67. Photograph of concretion in Anna Shale | 66 |
| 68. Sketch of Anna Shale subunits | 66 |
| 69. Photograph of concretions in Anna Shale exposed by roof fall | 67 |
| 70. Photograph of joints in Anna Shale | 67 |
| 71. Diagram of faults | 68 |
| 72. Photograph of Brereton Limestone forming stable roof | 69 |
| 73. Photograph of wedging relationship of rock layers in black shale-limestone roof | 70 |
| 74. Sketches of "washouts" | 70 |

| | | |
|------|---|-----|
| 75. | Photograph of Jamestown Coal above the Anna Shale | 72 |
| 76. | Photograph of Anna Shale and "Jamestown Coal interval" | 72 |
| 77. | Photograph of Conant Limestone with dolomitic concretions | 74 |
| 78. | Photograph of Jamestown Coal between well-developed Brereton and Conant Limestones | 74 |
| 79. | Photograph of horizons in the Lawson Shale | 76 |
| 80. | Photograph of syneresis cracks in the Lawson Shale | 76 |
| 81. | Photograph of unusual roof sequence above the Herrin (No. 6) Coal | 78 |
| 82. | Photograph of cross section of black shale-limestone roof sequence in strip mine | 78 |
| 83. | Computer-drawn map of the thickness of the Anna Shale in southern and southwestern Illinois | 80 |
| 84. | Computer-drawn map of the thickness of the Brereton Limestone Member in southern and southwestern Illinois | 81 |
| 85. | Computer-drawn map of the thickness of the Conant Limestone in southern and southwestern Illinois | 82 |
| 86. | Photograph of limestone "boss" | 84 |
| 87. | Photograph of syneresis cracks and mottled shale | 84 |
| 88. | Sketch of dessication fractures or syneresis cracks | 85 |
| 89. | Diagram of clay-dike faults | 86 |
| 90. | Photograph of a major clay-dike fault | 87 |
| 91. | Detail of figure 90 | 87 |
| 92. | Photograph of low-angle clay-dike faults | 88 |
| 93. | Diagram of clay-dike faults | 88 |
| 94. | Diagram of clay-dike faults | 88 |
| 95. | Diagram of orientation of clay-dike faults | 89 |
| 96. | Photograph of "goat beards" | 89 |
| 97. | Photograph of "goat beards" | 90 |
| 98. | Diagram of clay-dike faults dissipating into "goat beards" | 90 |
| 99. | Sketch of trends of low-angle normal faults | 90 |
| 100. | Diagram of low-angle normal faults displacing Anna Shale | 91 |
| 101. | Diagram of low-angle normal faults displacing Brereton Limestone | 91 |
| 102. | Diagram of low-angle normal faults displacing Lawson Shale strata | 92 |
| 103. | Diagram of low-angle normal faults displacing Herrin Coal and Anna Shale | 92 |
| 104. | Diagram of clay-dike faults forming graben and horst | 93 |
| 105. | Photograph of clay dike in Colchester (No. 2) Coal | 94 |
| 106. | Photograph of clay dike in Springfield (No. 5) Coal and roof strata | 95 |
| 107. | Photograph of clay-dike fault with thin clay filling | 96 |
| 108. | Diagram of clay-dike faults with clastic dikes in Herrin (No. 6) Coal | 97 |
| 109. | Diagram of clay-dike faults with clay dikes | 98 |
| 110. | Photograph of complex clay dike in Herrin (No. 6) Coal | 99 |
| 111. | Detail of figure 10 | 99 |
| 112. | Detail of figure 11 | 100 |
| 113. | Photograph of clay dike and clay-dike fault | 100 |
| 114. | Detail of figure 113 | 101 |
| 115. | Photograph of very low-angle clay dike fault | 101 |
| 116. | Map of elevation of the base of the Herrin (No. 6) Coal at mine A | 103 |
| 117. | Map of stations in study area 1 of mine A | 106 |
| 118. | Map of lithologic data of immediate roof in study area 1 of mine A | 108 |

| | | |
|------|--|-----|
| 119. | Map of roof lithology in study area 1 of mine A | 110 |
| 120. | Map of roof fall distribution in study area 1 of mine A | 112 |
| 121. | Map of clay dikes and clay-dike faults in study area 1 of mine A | 114 |
| 122. | Map of roof lithologies, structural features and roof falls in study area 1 of mine A | 116 |
| 123. | Map of additional data in study area 1 of mine A | 118 |
| 124. | Map of stations in study area 2 of mine A | 120 |
| 125. | Map of lithologic data of the immediate roof in study area 2 of mine A | 122 |
| 126. | Map of roof lithology in study area 2 of mine A | 124 |
| 127. | Map of roof fall distribution in study area 2 of mine A | 126 |
| 128. | Map of clay dikes and clay-dike faults in study area 2 of mine A | 128 |
| 129. | Map of roof lithologies, structural features and roof falls in study area 2 of mine A | 130 |
| 130. | Map of additional data in study area 2 of mine A | 132 |
| 131. | Map of elevation of the base of the Herrin (No. 6) Coal in study area 2 of mine A | 135 |
| 132. | Map of stations in study area 3 of mine A | 136 |
| 133. | Map of lithologic data of the immediate roof in study area 3 of mine A | 138 |
| 134. | Map of roof lithology in study area 3 of mine A | 140 |
| 135. | Map of roof falls in study area 3 of mine A | 142 |
| 136. | Map of clay dikes and clay-dike faults in study area 3 of mine A | 144 |
| 137. | Map of roof lithologies, structural features and of roof faults in study area 3 of mine A | 146 |
| 138. | Map of additional data for study area 3 in mine A | 148 |
| 139. | Geologic map of study area 4 of mine B | 153 |
| 140. | Map of roof lithologies, rolls and roof falls of study area 5 of mine B | 154 |
| 141. | Map of shear body, roof lithologies, and roof falls in study area 5 of mine B | 156 |
| 142. | Computer-generated map of elevation of the top of the Herrin (No. 6) Coal in study area 5 of mine B | 158 |
| 143. | Computer-generated map of elevation of the top of the Herrin (No. 6) Coal in the region of study area 5 of mine B | 159 |
| 144. | Computer-generated map of the top of the Herrin (No. 6) Coal in study areas 6 and 7 of mine C | 160 |
| 145. | Map of roof lithology and roof falls in study area 6 of mine C | 161 |
| 146. | Sequential maps of roof-fall development in study area 6 of mine C | 162 |
| 147. | Map of roof lithology in study area 7 of mine C | 163 |
| 148. | Map of roof falls in study area 7 of mine C | 164 |
| 149. | Map of elevation of the top of the Herrin (No. 6) Coal Member in the "Quality Circle" area | 168 |
| 150. | Map of thickness trends of the Energy Shale Member in the "Quality Circle" area | 168 |
| 151. | Map of thickness trends of the Anna Shale Member in the "Quality Circle" area | 169 |
| 152. | Map of thickness trends of the Brereton Limestone Member in the "Quality Circle" area | 169 |
| 153. | Map of elevation of the top of the Herrin (No. 6) Coal Member in Bond and Montgomery Counties | 170 |
| 154. | Map of thickness trends of the Anna Shale Member in Bond and Montgomery Counties | 170 |

| | | |
|------|---|-----|
| 155. | Map of thickness trends of the Brereton Limestone Member in Bond and Montgomery Counties | 171 |
| 156. | Map of thickness trends of the interval from the Herrin (No. 6) Coal to the first thick limestone bed in Bond and Montgomery Counties | 171 |
| 157. | Thickness trends of the interval from the Herrin (No. 6) Coal to the first thick limestone bed in southwestern and southern Illinois | 172 |
| 158. | Schematic of roof falls due to rolls in gray shale roof | 173 |
| 159. | Schematic of roof fall in laminated siltstone and sandstone roof | 174 |
| 160. | Schematic of roof fall in wet zones in Energy Shale roof | 174 |
| 161. | Schematic of roof fall in limestone roof | 174 |
| 162. | Schematic of roof fall in black shale roof | 174 |
| 163. | Graph of compressive strength of rocks as a function of Young's modulus | 180 |
| 164. | Graph of peak and residual frictional coefficients for shales | 182 |
| 165. | Graph of compressive strength as a function of deformation modulus of coals | 182 |
| 166. | Graph of moisture-density relation in shales and underclays | 182 |
| 167. | Graph of moisture-density relation in shales | 182 |
| 168. | Graph of moisture content as a function of compressive strength of shales | 183 |
| 169. | Graph of moisture content as a function of deformation modulus of shales | 183 |
| 170. | Graph comparing deformation modulus with compressive strength of shales | 183 |
| 171. | Graph comparing undrained deformation modulus with undrained compressive strength of shales | 183 |
| 172. | Graph comparing undrained deformation modulus with undrained compressive strength of shales and underclays | 184 |
| 173. | Photograph showing effects of water on degree of slake durability and amount of disaggregation of shales | 187 |
| 174. | Radiograph of a well-bedded fissile portion of shale | 189 |
| 175. | Radiograph of a mottled gray shale | 189 |
| 176. | Radiograph of a well-bedded argillaceous siltstone and silty shale | 190 |
| 177. | Schematic of the relationship of roof lithology to coal topography | 192 |
| 178. | Diagram of room-and-pillar layout in faulted areas | 197 |
| 179. | Diagram of roof fall of Energy Shale in mine Q | 197 |

INTRODUCTION

Every year roughly half the injuries in American coal mines are caused by falls of roof and rib. The geologic composition of roof rock strata has an important bearing on the stability of roof and rib, but the relationship is poorly understood. Therefore, the U.S. Bureau of Mines has supported a number of studies on the influence of geologic factors on roof stability.

The Illinois State Geological Survey has collected data that applies to such research, but this study is more systematic and intensive than any previously attempted. The financial support of the U.S. Bureau of Mines (contract no. H0242017) between 1974 and 1976 allowed the research that is reported here. Roof studies continue to receive high priority in the Survey's coal-related programs.

The Herrin (No. 6) Coal was the most appropriate for this study because it provides roughly 80 percent of the state's current coal production and almost half of the coal resources of Illinois. Most of this coal (85 to 90 percent) lies at depths greater than 150 feet (50 m) and can be recovered only by underground mining.

Objectives of this study were to find and describe the geologic factors that influence roof conditions in underground mines. The primary method of study was detailed mapping in mines, supplemented by regional computer mapping using drill-hole data, close-range photogrammetry, physical testing of core samples, and clay mineralogical investigations of roof material.

Over a period of three years, a large volume of data has been generated. The results are therefore reported in two volumes. Volume 1 is a summary for general use of the major findings and conclusions. Volume 2 includes a detailed account of the method of study, the data gathered, and the conclusions reached.

The geologic setting of the Illinois Basin Coal Field

The Illinois Basin Coal Field covers more than 65 percent of the state of Illinois, along with adjacent portions of southwestern Indiana and western Kentucky. All commercial coal in the Illinois Basin Coal Field

occurs in strata of the Pennsylvanian System. In Illinois, 92 percent of the identified resources lie in the Carbondale Formation (fig. 1). The Herrin (No. 6) Coal Member of the Carbondale Formation accounts for 42 percent of the coal resources and 80 percent of the current production in Illinois (Smith and Stall, 1975).

The Herrin (No. 6) Coal subcrops around the margin of the Illinois Basin Coal Field and attains a maximum depth of about 1300 feet (about 400 m) in the Fairfield Basin (fig. 2) in Wayne County (Allgaier and Hopkins, 1975). The coal dips gently toward the center of the basin and is essentially flat-lying through most of its range. Inclination rarely exceeds 1 to 2 percent except along the La Salle Anticlinal Belt in eastern Illinois, the Du Quoin Monocline, and the Cottage Grove Fault System in southern Illinois, where dips exceeding 15 degrees have been recorded.

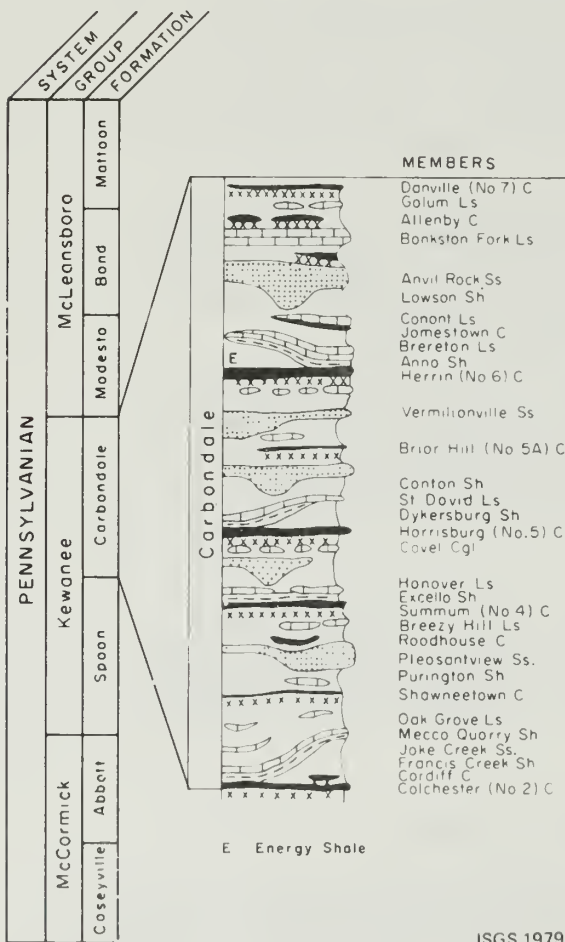


Figure 1. Stratigraphic section of the Carbondale Formation, Kewanee Group, showing the positions of the most important coals within the Pennsylvanian System in Illinois. (After W. H. Smith, 1975.)

The Herrin (No. 6) Coal is the most widespread coal in Illinois and exceeds a thickness of 60 inches (1.52 m) over broad areas (fig. 3). The coal rank has been determined to be high-volatile A, B, and C bituminous and has a sulfur content normally varying from 3 to 5 percent. In the "Quality Circle" area of Franklin and Williamson Counties in southern Illinois (fig. 3), a maximum coal thickness of about 14 feet (4.3 m) has been reported, and the sulfur content ranges from less than 1 to 2 percent. Some of this low-sulfur coal is of the quality used for manufacturing metallurgical coke in blends with higher-ranked coal.

The general sequence of rocks overlying the Herrin (No. 6) Coal is shown in figure 4. Although a wide variety of lithologies and deposits of various geologic environments are represented, two major roof rock assemblages have been studied in detail. One is the gray shale roof type comprising the Energy Shale

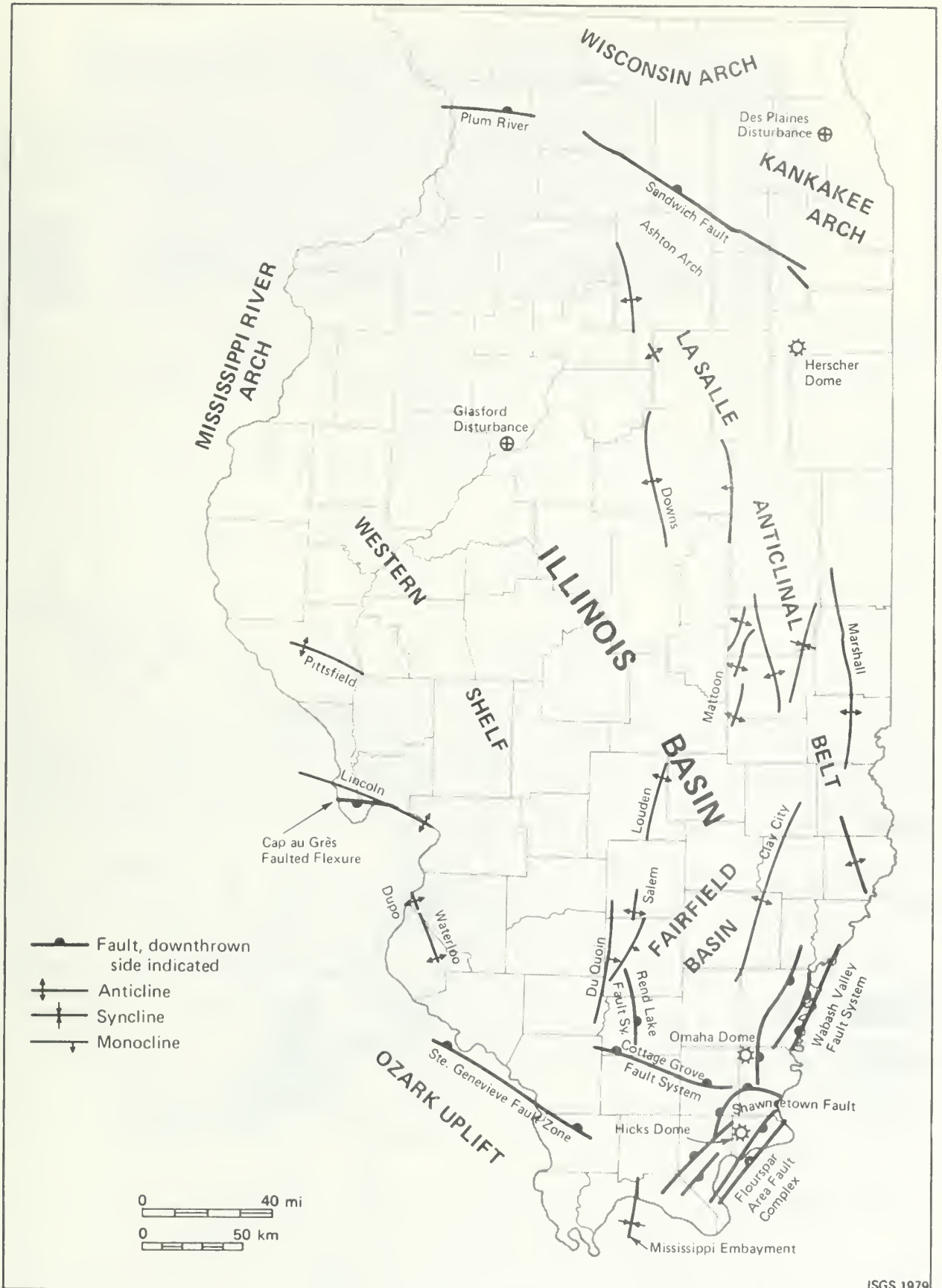


Figure 2. Geologic structures of Illinois.

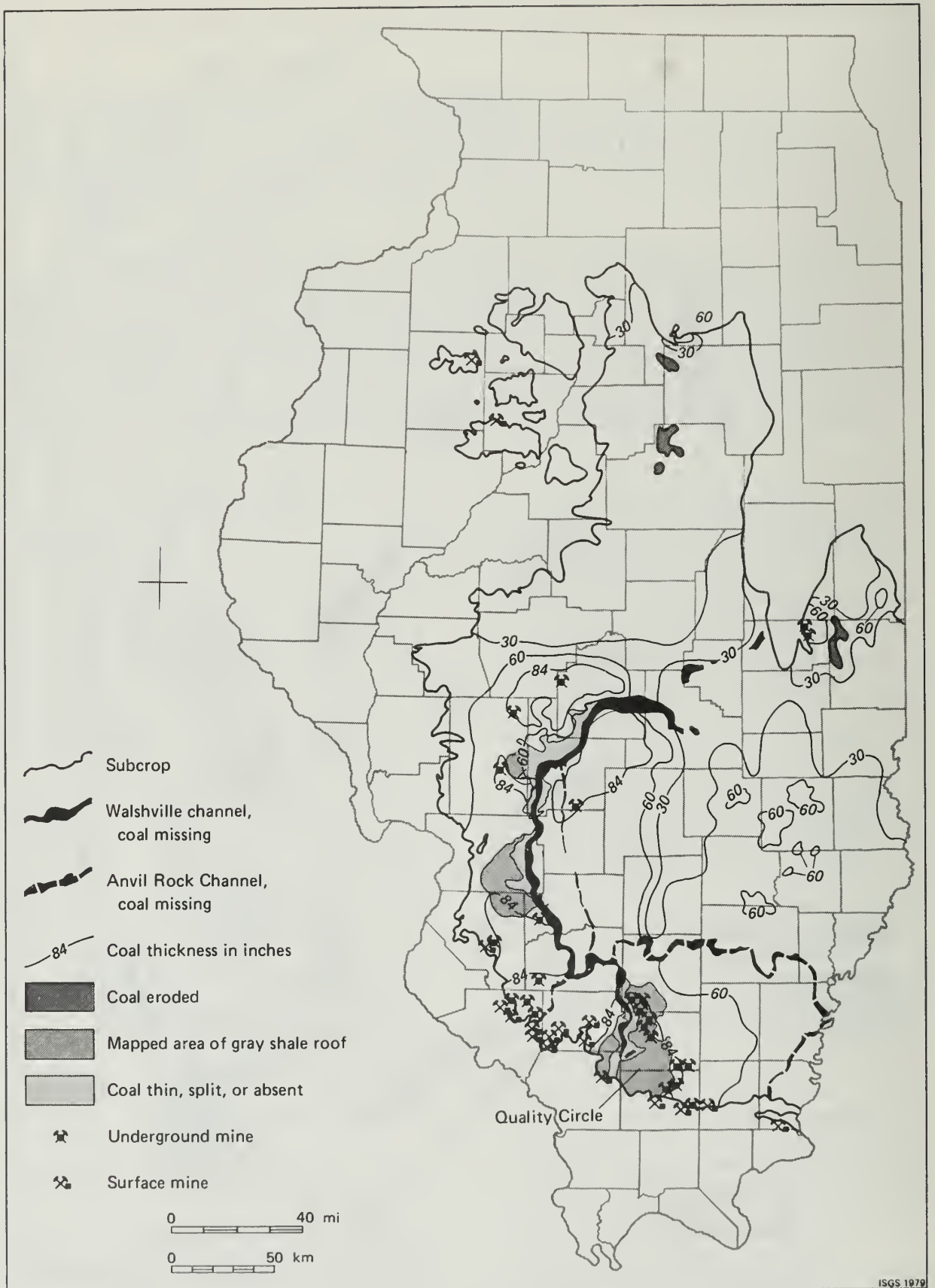


Figure 3. Distribution of the Herrin (No. 6) Coal in Illinois.

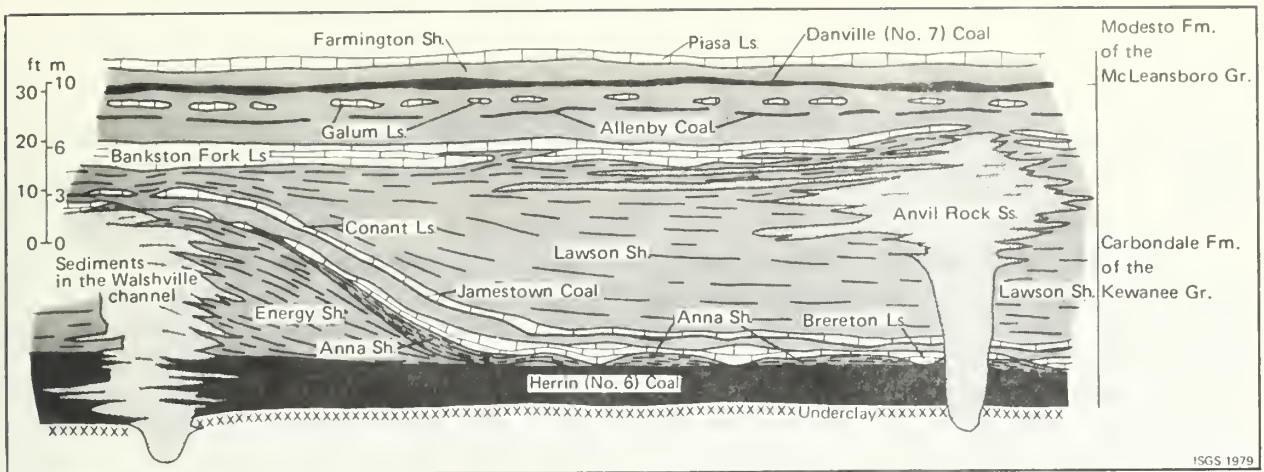


Figure 4. Schematic section of the interval between the Herrin (No. 6) Coal Member and the Piasa Limestone Member. (After G. J. Allgaier, June 1974.)

Member and the sandstones, siltstones, and shales in the Walshville channel (left side, fig. 4). The other roof type is the black shale-limestone roof type, an assemblage including the Anna Shale Member and overlying units (right side, fig. 4). Distinctive lithologic and structural assemblages and a variety of mining and roof conditions are associated with the two major roof rock types.

The sediments of the Energy Shale associated with the Walshville channel form the gray shale roof type. They are believed to be deposits of a major river system that existed contemporaneously with peat accumulation. In the Walshville channel itself, the Herrin (No. 6) Coal is absent. Along the channel margins the coal is generally split. Flanking the channel, the coal is overlain by gray shale, siltstones, and sandstones of the Energy Shale Member. The Energy Shale attains a maximum thickness of about 100 feet (30 m) and laterally decreases in thickness away from the Walshville channel. Overlying the Energy Shale are marine strata of the black shale-limestone roof type, which tend to be lenticular or pinch out as the Energy Shale thickens. Where the Energy Shale is absent, the black shale-limestone sequence forms the immediate coal roof.

A close interdependence exists between the sulfur content of the coal and the characteristics of overlying strata. Where the nonmarine Energy Shale is more than about 20 feet (6 m) thick, the coal has a relatively low content of sulfur. This relationship has been observed in several areas and is particularly notable in the "Quality Circle" area of southern Illinois. It is supposed that the Energy Shale represents crevasse-splay and overbank deposits from the river that formed the Walshville channel and that the

deposits covered the coal-forming plant material before marine ingression and protected it against emplacement of sulfur (Gluskoter and Hopkins, 1970).

The black shale-limestone roof type includes seven named stratigraphic rock members relevant to mine roof stability (fig. 4). All are highly persistent regionally, but show considerable local variability. The lowest member is the Anna Shale Member, typically a black, carbonaceous, phosphatic, fissile shale, rarely exceeding 5 feet (1.5 m) in thickness. The Anna Shale is thought to represent deposition in shallow lagoonal environments. Overlying is the Brereton Limestone Member, a generally fine-grained, argillaceous, fossiliferous rock representing more open marine conditions. In southwestern Illinois, its thickness may exceed 18 feet (5.5 m), but 4 to 5 feet (1.2 to 1.5 m) is more common. The Jamestown Coal Member is thin but widespread in most of Illinois, increasing to minable thickness in extreme eastern Illinois and western Indiana. Where the Jamestown Coal is thin, the interval between the underlying and overlying members includes not only coal, but also a distinctive dark-gray carbonaceous shale containing nodules of chert and small lenses of medium-gray limestone, probably of freshwater origin. This interval is referred to as the "Jamestown Coal interval" in this study.

The overlying Conant Limestone Member appears to be lithologically similar to the Brereton Limestone; however, it is thinner, about 6 feet (1.8 m) at maximum, but typically less than 1.5 feet (0.32 m). Next in sequence are the Lawson Shale and the Anvil Rock Sandstone Members, highly heterogeneous facies equivalents. They include generally mottled, greenish shales and claystones; locally calcareous shale with marine fossils; firm, gray, silty shales; siltstones; sandstones; and, in places, conglomerates. A well-developed channel system of the Anvil Rock Sandstone has been mapped in which underlying strata locally including the Herrin (No. 6) Coal were eroded. Channels filled by Anvil Rock Sandstone are shown in figure 3.

The highest stratigraphic member exposed in many roof falls of underground mines is the Bankston Fork Limestone. Most often it consists of several benches of light-gray to buff, fine-grained, nodular limestone, interstratified with one or more bands or layers of mottled greenish shale or claystone. Its fauna of mainly brachiopods and fusulinids demonstrates open-marine environment of deposition.

Techniques employed

A variety of techniques have been employed to analyze and describe the relationship between geologic conditions and mine-roof stability, including:

1. Detailed geologic mapping within selected study areas in underground mines
2. Regional computer mapping using drill-hole data
3. Close-range photogrammetry

4. Core drilling in underground mines
5. Laboratory testing of drill cores
6. Clay mineralogy studies

The in-mine mapping was the most significant and also most time-consuming work performed in this study. Seven selected study areas in three underground coal mines were mapped in detail. The base maps, generally at a scale of 1:1200, were provided by the mining companies. Within each mapping area all accessible mine headings were walked, and all features were plotted directly on the base maps. The features mapped included all geologic structures such as faults, joints, rolls, and clay dikes; the lithology of the immediate roof; the observed sequence of roof strata; and the roof falls. Various combination and compilation maps were prepared from the field maps.

Regional computer mapping was applied to 23 counties where reserves of the Herrin (No. 6) Coal are significantly large (fig. 5). Data on thickness and elevation were evaluated for all rock units from the Herrin (No. 6) Coal



Figure 5. Area in the southern half of Illinois for which data on thickness and facies of roof strata above the Herrin (No. 6) Coal extending up to the Piasa Limestone were collected and compiled in computer-processible form.

through the Piasa Limestone Member (fig. 4), using thousands of core descriptions, drillers' logs, and geophysical logs from the drill-hole record library at the Illinois State Geological Survey (ISGS). An average of about one hole for each two square miles was used. The maps were computer-generated using GEOMAPS, a program package developed by the Illinois State Geological Survey from ILLIMAP (Swann et al., 1970), and STAMPEDE (IBM Corp., 1968).

Maps generated include structural contour maps of the top or base of the coal, maps showing thicknesses of the significant roof rock units, and maps showing thicknesses of particular rock intervals of specific interest for the study, such as the interval from the top of the coal to the base of the first competent limestone bed. In addition, the computer was employed to produce structural contour maps of coal seams at the mines selected for detailed mapping.

A close-range photogrammetric technique was developed to collect information on orientation of cleats, joints, and shear planes in areas that were too steep or dangerous for direct approach and measurements. It was also used to map an advancing strip-mine highwall to obtain a three-dimensional picture of the shape of roof rock bodies. (Details on photogrammetry are presented in volume 2 and in Brandow et al., 1975).

A limited amount of core in underground mines was drilled to obtain fresh samples for testing unconfined compressive strength and Young's modulus. A total of six cores were taken: three of roof rock, one horizontal core of coal, and two horizontal cores of a large sandstone roll.

A variety of mechanical, optical, chemical, radiographical, and x-ray diffraction analyses were performed for clay-mineralogy studies of roof and floor shales. Rock properties tested included grain and particle size, clay mineralogy, Atterberg limits, slake durability, orientation of clay minerals, texture, and internal structure. Details are presented in volume 2.

ROOF TYPES OF THE HERRIN (NO. 6) COAL MEMBER IN ILLINOIS

Two major roof types overlie the Herrin (No. 6) Coal in Illinois. The gray shale roof type comprises primarily gray, nonmarine sandstones, siltstones, and shales of the Energy Shale Member. The black shale-limestone roof type includes both marine and nonmarine deposits of the Anna Shale and overlying stratigraphic units. A third type is transitional, having components of both gray shale and black shale-limestone roof types. For this investigation, we designated study areas 1 through 3 (in mine A) under black shale-limestone roof and study areas 4 and 5 (in mine B) and 6 and 7 (in mine C) under gray shale roof for detailed examination and mapping. No transitional roof areas were mapped or studied closely.

The gray shale roof type and the black shale-limestone roof type are distinct lithologically and each contains unique and distinctive structural deformation features. These associations between structure and lithology lead to specific patterns of mine roof stability for each roof type.

Gray shale roof types

Three distinct dominant facies of the Energy Shale were recognized and mapped:

1. Dark-gray shale facies (at base)
2. Medium-gray shale facies
3. Planar-bedded siltstone and sandstone

The dark-gray shale facies is the lowest stratigraphically, forming the immediate roof in large areas of mine B. Its thickness ranges from zero to five feet (0 to 1.5 m) and is most commonly less than two feet (0.6 m) thick. It is conformably overlain by medium-gray shale. The dark-gray shale ranges from medium-dark gray to almost black; its dark color results from abundant, finely dispersed, carbonaceous debris. It is hard, smooth, and generally laminated. The presence of fossils, including small pelecypods and *Anthracosiidae*, indicates a deposit in fresh to brackish water.

Jointing in the dark-gray shale generally is much more regular and closely spaced than in the other Energy Shale facies. The dark-gray shale is variable with regard to roof stability. Over wide areas it is stable, but in some places, where it acts as a "draw slate," roof falls can occur, particularly where the shale is thick.

Medium-gray shale is the dominant facies of the Energy Shale. It overlies the dark-gray shale in mine B and forms the immediate roof in much of mine C. Medium-gray shale may attain thicknesses of 50 feet (15 m) or more. It contains much less carbonaceous material than the dark gray shale, and laminations and joints are distinctive or absent. In some places mica and plant debris coating the bedding planes permit the mine roof to separate in layers and to break in large slabs, but elsewhere the rock is a massive mudstone that forms a stable roof, except where structural anomalies or deformational features are present. The medium-gray shale is susceptible to moisture slaking, and over long periods of time large falls may develop, although the shale generally is stable.

The medium-gray shale may grade both laterally and vertically into silty shale, siltstone, and sandstone; however, the planar-bedded siltstone and sandstone mapped in mine C is a distinct facies that was deposited adjacent to the Walshville channel. It overlies the medium-gray shale with a sharp, apparently unconformable contact, and in part of the study area the shale is absent and sandstone rests directly on the coal.

The planar-bedded siltstone and sandstone is marked by closely spaced regular partings of coarse mica and carbonaceous plant debris on bedding surfaces. The rock easily splits and separates along those partings, and spectacular roof falls are common (fig. 6). In addition, the sandstone may contain water, which weakens the underlying medium-gray shale and promotes more falls; the seepage or flow of water into mining areas causes serious problems.

Any of the Energy Shale facies described may be underlain by a basal carbonaceous layer containing abundant coalified plant debris, including some that may be hazardous to miners, such as fossilized tree stumps, whose cores may fall out of the roof. The entire basal layer is generally unstable, but is thin enough (less than a foot) to be relatively unimportant to overall roof stability.

Rolls, protrusions of roof material into coal, are the most typical and widespread structural features of coal and roof in areas where the gray shale overlies the coal. Most rolls are elongate, linear features shaped roughly like footballs in cross section (fig. 7). The length of rolls may reach several hundred feet, the width ranges from a few inches to about a hundred feet, and thickness ranges from a few inches to the height of the coal seam. Most rolls observed in our studies are asymmetrical and have a blunt "toe" along which a splayed-out coal "rider" curves upward into the roof. At the "tail" end of the roll, coal riders are poorly developed, but large slickensided compactional faults are common. The combination of coal riders and faults seriously weakens the roof above the main body of the roll, which may break down as soon as it is undermined.

Rolls are abundant in areas of medium-gray shale and planar-bedded siltstone and sandstone roof, but they are small and rare where dark-gray shale forms the immediate roof. The lithologic material of the roll is usually the same as the material forming the roof above the roll. The interior bedding of the roll commonly is distorted, especially at and near the "toe" of the roll. The rolls in figures 8 through 12 are typical.

Rolls at mine B tend to strike parallel with boundaries between medium-gray shale and dark-gray shale (figs. 13-15). A pattern of sandstone rolls in mine C is less apparent, but there is a general trend for rolls to strike parallel to the edge of the sandstone roof area (fig. 16).

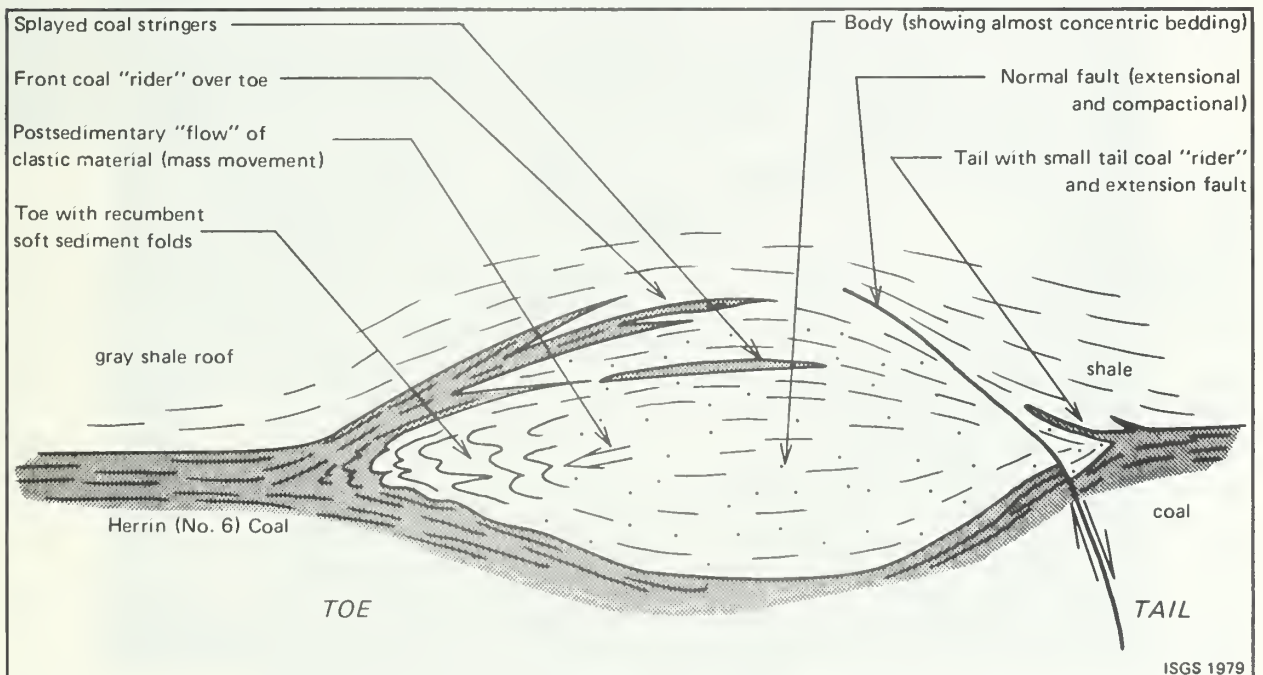
The internal structure and mapped distribution and orientation of rolls suggest that they are load structures that formed as slump features in which soft sediments squeezed into the upper layers of the coal-forming material. No indications of coal erosion have been found that indicate the rolls originated as in-filled stream channels.

Slips and small faults not associated with rolls are common throughout the mapped areas in the gray shale roof type. The maximum displacement along these small faults is two to three feet (0.6 to 0.9 m), but commonly it is much less. Generally, small faults die out within the coal seam, and rarely do they extend far into the roof strata. Their orientation may be roughly parallel to boundaries of facies-changes, but in contrast to those in the black shale roof type, many of the slips and small faults in the gray shale roof type show no preferred orientation. All indications are that these slips resulted from differential compaction of the sediments. Slips and small faults locally may be a roof hazard, especially where two or more intersect above the coal seam.

A large body of pervasively sheared roof rock was encountered in study area 5, mine B (fig. 15). This rock body, herein termed a "shear body," is more than 2500 feet (760 m) long, 200 to 300 feet (60 to 90 m) wide, and at least 30 feet (9 m) thick. It is irregular in outline, trending roughly east and west through the study area. The lower boundary is a series of shear planes (figs. 17, 18) that are almost parallel to bedding and lie on or close to the top of the coal in the heart of the shear body. They curve upward into the roof along its margins. The coal and rock below the shear body are almost undeformed. The formation of the shear body postdates formation of rolls, as indicated by truncation of the tops of rolls by the shear body (fig. 19).



Figure 6. Roof fall in planar-bedded sandstone of the Energy Shale Member. Bedding surfaces are coated with mica and coalified plant fragments. No prominent joints are visible. Sandstone failed and broke almost straight up along the pillar rib. Location: "Quality Circle," near Walshville channel, mine C.



ISGS 1979

Figure 7. Sketch of typical roll (soft-sediment protrusion of clastic materials into surrounding sediments—coal, shales, siltstones, and sandstones).



Figure 8. Roll of medium-gray shale of the Energy Shale Member intruded into top layers of the Herrin (No. 6) Coal. Toe (at the left) splits folded coal strata into several stringers. Tail has been truncated by compactional normal fault (at the right). The rod is about 4 feet (1.2 m) long. Location: "Quality Circle."



Figure 9. Large roll (10 feet [3 m] wide) of siltstone material. The toe of the roll displays slight soft-sediment deformation. Coal "rider" extends over two-thirds of the roll. Location: "Quality Circle," southern Illinois, mine C.

Figure 10. Roll in planar-bedded siltstone and sandstone of the Energy Shale Member. Near the toe of the roll (arrow), recumbent soft-sediment folds and low-angle shear planes are visible. These features suggest that the silt and sand filling the roll intruded from right to left between the layers of peat. (Note the coal "rider" originating at the toe and extending almost entirely over the roll.) The large low-angle slips at the tail of the rolls may have formed later by differential compaction.

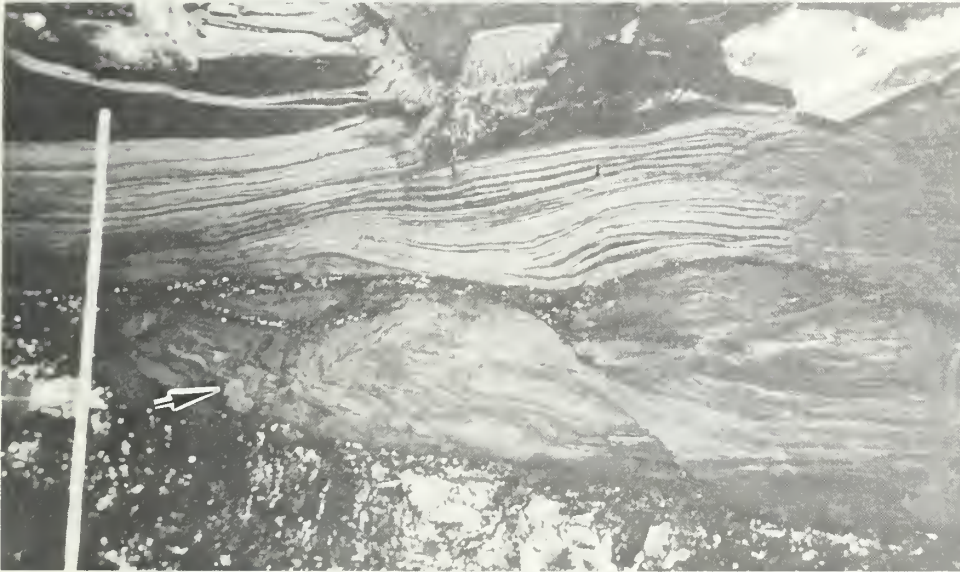


Figure 11. Detail of figure 10.

Figure 12. Detail of figure 11.



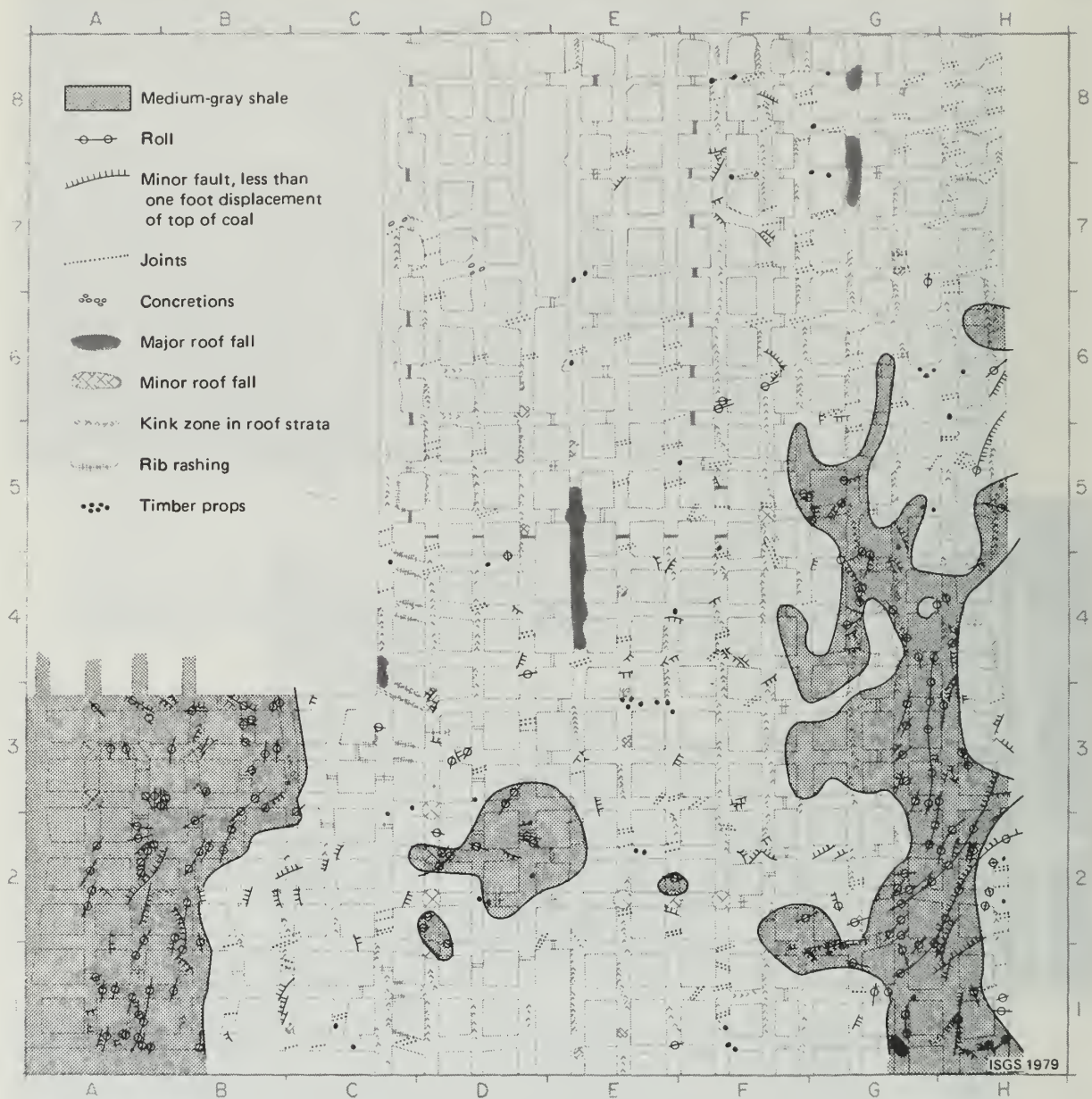


Figure 13. Lithology, structural features, and roof falls of the Herrin (No. 6) Coal and its immediate roof rocks in study area 4, mine B. The immediate roof strata are Energy Shale, lower portion (not stippled) dark-gray shale and upper portion (stippled) medium-gray shale. The majority of rolls and faults occur in medium-gray shale, whereas all but one of the roof falls and other features of instability (e.g., kink zones and rib rashing) are distributed in areas of dark-gray shale. Jointing is also much more prominent in the well-bedded dark-gray shale. Grid interval is 200 feet (61 m).

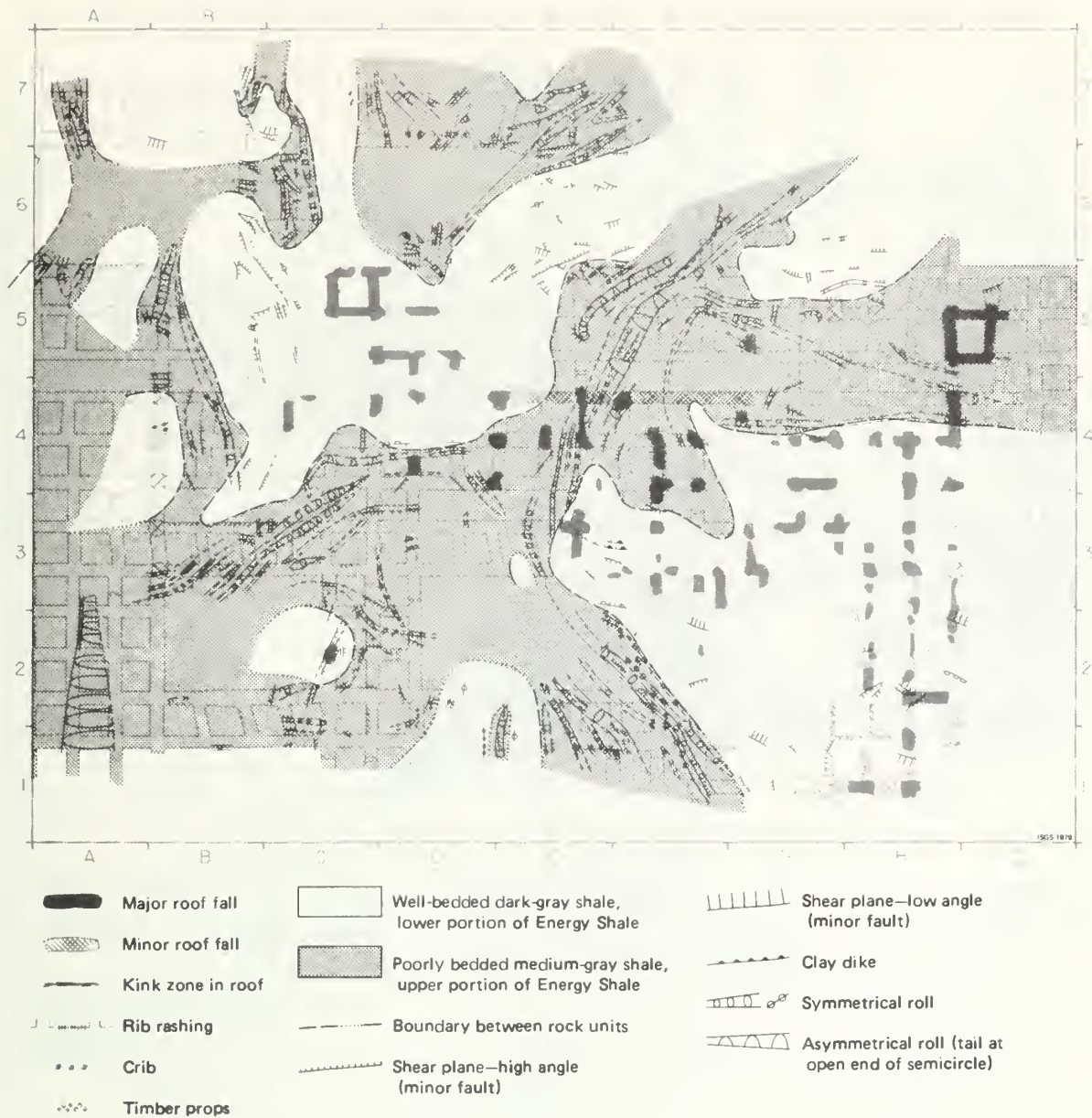


Figure 14. Distribution of soft-sediment rolls with associated minor faults in relation to the lithology of the immediate roof and roof falls of Herrin (No. 6) Coal in study area 5, mine B. The map displays the close interdependence of soft-sediment structural features, mainly rolls and slips, with the distribution and lateral boundaries of the Energy Shale roof strata. Although the immediate roof in areas of medium-gray shale with rolls and slips commonly is very rough and irregular, the roof falls are more abundant in areas of dark-gray shale. Roof falls in areas of medium-gray shale occur mainly within the shear body. Grid interval is 200 feet (61 m).

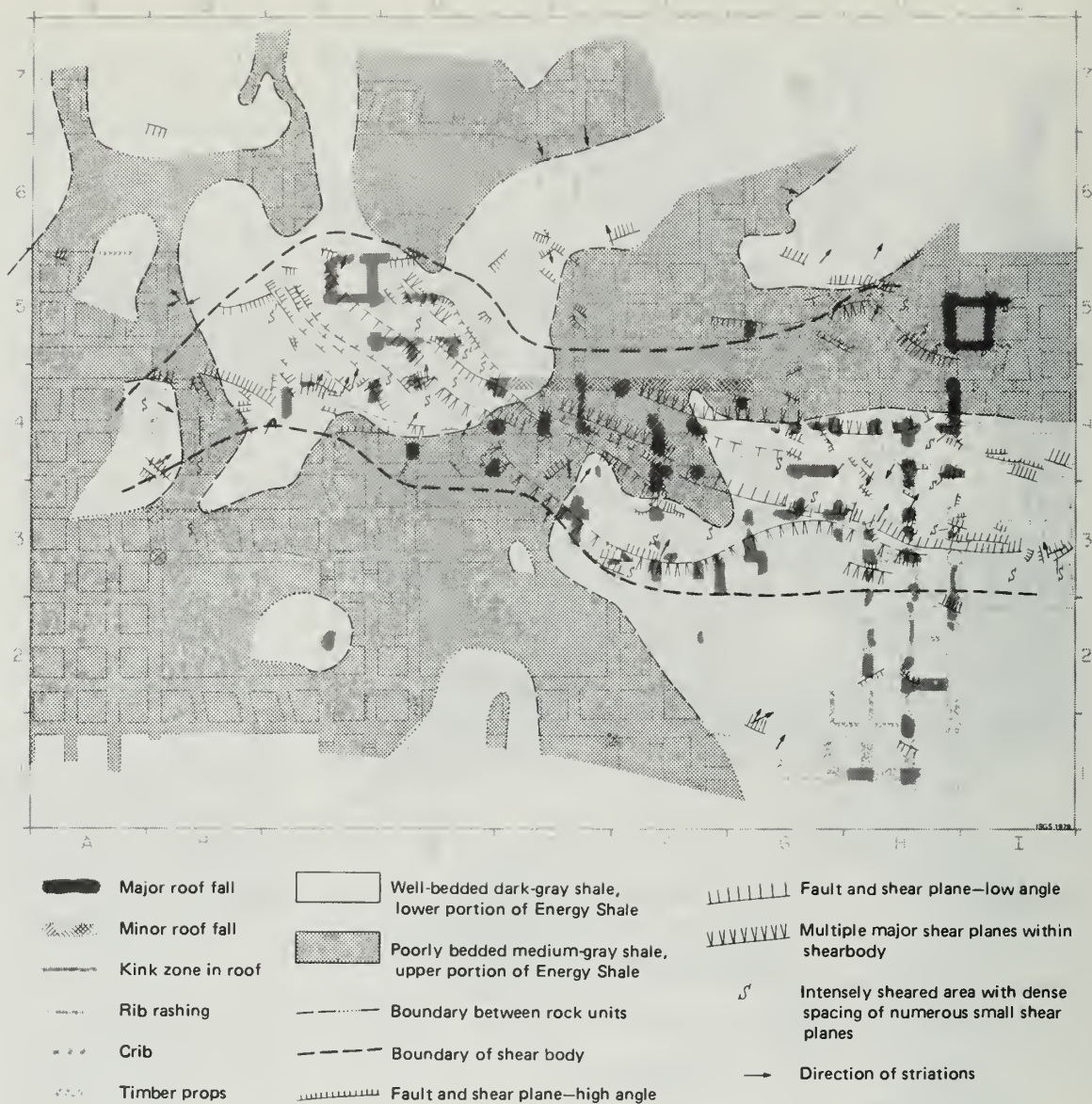


Figure 15. Outline and major shear structures of the shear body in study area 5, mine B. Roof falls have occurred most often in the area of the shear body and to a lesser degree under dark-gray shale, in the immediate vicinity of the shear body. Deformational features older than the shear body have not been drawn on this map, but can be compared in their interrelationship to lithologic differences in figure 14. The shear body is not restricted to a particular lithology but affects dark-gray shale and medium-gray shale and, locally, the top of the Herrin (No. 6) Coal as well. Grid interval is 200 feet (61 m).

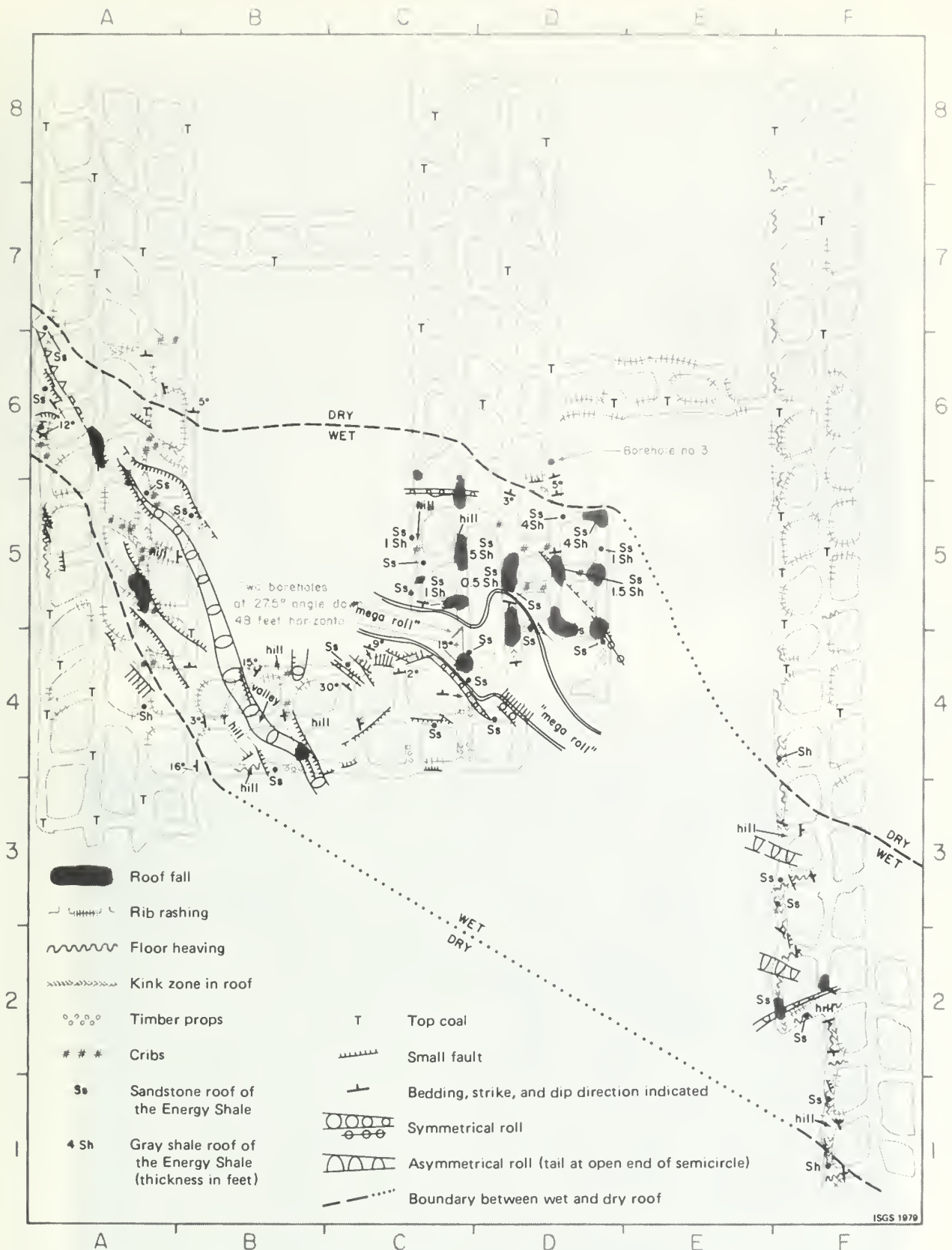


Figure 16. Lithology, rolls, and fault structures of the Herrin (No. 6) Coal and its immediate roof strata and the distribution of roof falls, other induced instabilities, and additional roof support (timber and cribs) in the area below siltstone and sandstone with water seepage (wet). Study area 7, mine C. Grid interval is 200 feet (61 m).



Figure 17. Almost undisturbed Herrin (No. 6) Coal and some beds of finely laminated silty shale truncated by a northward-dipping (to the left) set of major shear surfaces and overlain by the shear body. Location: southern Illinois, "Quality Circle," study area 5, mine B.



Figure 18. Detail of figure 17—major shear surfaces, a set of very low-angle normal faults bordering the shear body (light rock, upper part of photo) and truncating finely laminated shale below. Note the associated drag folds (soft-sediment folds above compass) within the shear zone.

Within the shear body, a peculiar deformational facies of rock has developed. The dominant lithology is soft, greenish claystone or altered shale having highly contorted bedding, intensely sheared. Also found are blocks and layers of finely laminated, microfaulted siltstone or sandstone (figs. 20, 21), brecciated dark-gray shale with siderite, and blocks of bony coal. Nothing similar has been found in any other study area. This deformational facies is penetrated by a great number of horizontal to gently dipping slickensided shear surfaces.

Roof failures in the shear body are abundant. As shown in figure 15, many roof falls have developed in the shear body and along its margins. The average height of falls is 15 to 20 feet ($4\frac{1}{2}$ to 6 m). Entries essential for haulage, air, and travel could be kept open only by additional support such as massive cribbing and steel beams. Roof bolts did not sufficiently anchor in the intensively sheared rock, and failed.

Although this is the first shear body ever to be described in strata above the Herrin (No. 6) Coal, there is no reason to assume it is unique. Its origin is believed to be the result of gravitational sliding. Similar features have been described for other regions (Potter, 1957, and Voigt, 1969).

Significant jointing is encountered only in the dark-gray shale facies at mine B. The joints strike $N 60^{\circ}$ to $80^{\circ}E$ and generally penetrate less than one foot vertically into the roof. Their spacing is generally about five to ten joints per foot. These joints may contribute to slabbing of the immediate roof, but generally do not cause major roof falls.



Figure 19. Nearly horizontal shear zone of a set of shear surfaces enclosing dragged, folded, and sheared dark-gray shale; main shear movement of each upper shear bed is toward the left and has truncated the top of a major roll of silty medium-gray shale. This indicates that formation of shear body continues after or even postdates formation of rolls; however, small low-angle antithetic faults truncate shear zone of dark-gray shale and remnant of rolls, so these postdate both roll and shear zone. Section from bottom of photo to top: (A) coal slightly deformed by fault in roll (left side of photo), (B) laminated silty shale within the roll, (C) folded, sheared, and intensely contorted dark-gray shale in shear zone, and (D) greenish claystone of main shear body. Scale: holes in aluminum frame are one foot (30.5 cm) apart. Location: southern Illinois, "Quality Circle," study area 5, mine B.

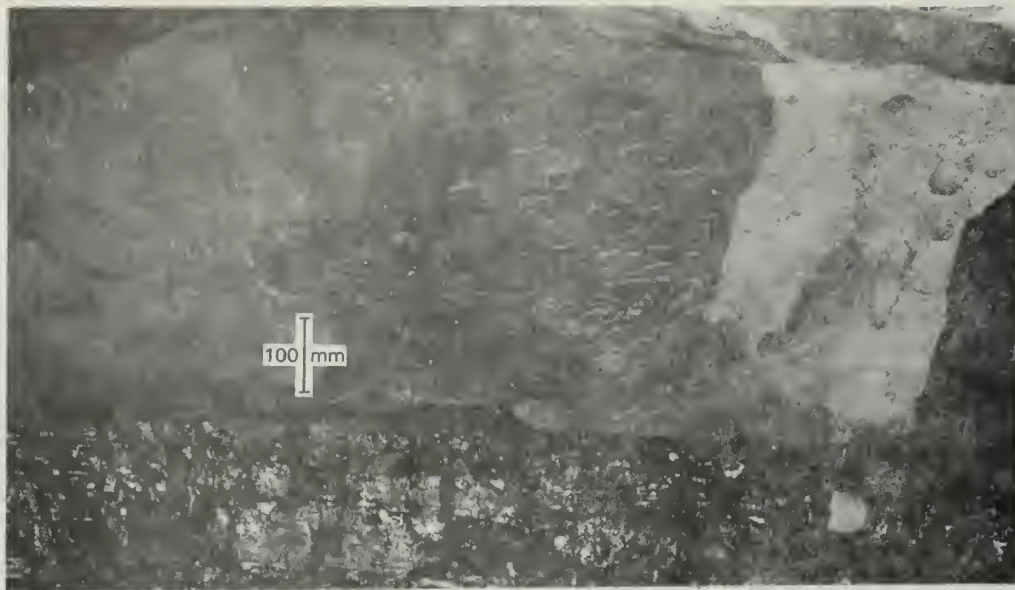


Figure 20. Microfaulted laminated silty shale and siltstone. Low-angle and high-angle shear planes are adjacent and are of a single deformational action. The microfault pattern resembles the lower portion of seismites described by Seilacher (1969). Mass movement in general is downward, and each lower portion has moved laterally toward the south (left in photo). Major shear plane is subparallel to bedding just above coal. Coal itself is affected only at extreme top. Location: southern Illinois, "Quality Circle," study area 5, mine B.



Figure 21. Detail of figure 20.

In study area 4, mine B (fig. 13) roof falls and kink zones have a strong tendency to extend in a north-south direction. (Kink zones are narrow zones of compressional cracking and sagging which develop in the immediate roof after mining.) The cause of this north-south weakness is not known, but it should be noted that it trends parallel with the Rend Lake Fault System that passes about 1000 feet (300 m) west of the study area.

Black shale-limestone roof types

Three areas having the black shale-limestone roof type were mapped in mine A. This roof type was also examined in less detail at several other surface and underground mines. The geologic and roof control problems in the black shale-limestone roof type differ considerably from those found in gray shale roof.

The generalized roof rock sequence at mine A is shown in figure 22. The lowest stratigraphic member is the Anna Shale, which reaches a maximum thickness of five feet (1.5 m) and is usually two to three feet (0.6 to 0.9 m) thick; however, the Anna Shale may be absent locally.

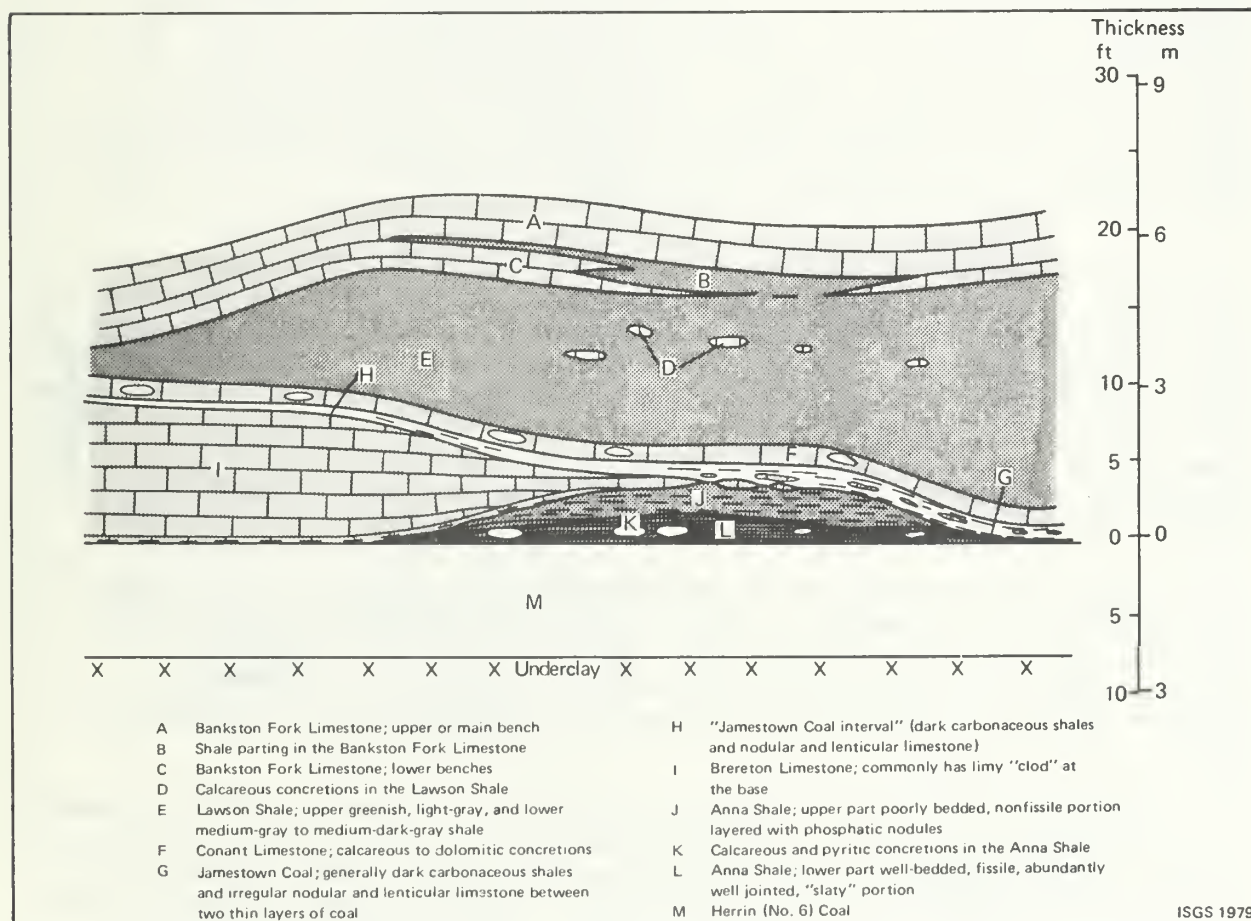


Figure 22. Black shale limestone roof; sequence of rock stratigraphic members at mine A.

Two distinct subunits of the Anna Shale have been recognized at mine A. The lower subunit is black, hard, fissile, "slaty" shale, significantly well jointed and containing large spheroidal concretions. The upper subunit consists of a poorly bedded, mottled, weak shale containing two persistent thin bands of phosphatic nodules. Where the Anna Shale is less than one foot (0.3 m) thick, the entire member is fissile. Where the Anna Shale is more than one foot thick, it shows both subunits in most cases.

The Anna Shale generally is a firm roof material, although the lower layers tend to slab along joint planes. Concretions pose a local hazard that can be countered by pulling them down or bolting through them. Local roof falls to the base of the overlying limestone occur where the upper mottled subunit is not strong enough to be self-supporting; however, large roof falls in the Anna Shale do not result from its lithologic composition alone, but are related to slips, minor faults, and densely spaced joints that penetrate the entire Anna Shale and add to other structural weaknesses.

Overlying the Anna Shale, or forming the immediate roof where the Anna Shale is absent, is the Brereton Limestone. This member is the key to roof stability at mine A. Where it forms the immediate roof, it is five to more than ten feet (1.5 to >3 m) thick, and roof falls are practically unknown (figs. 23-25). The basal "clod" layer, consisting of a few inches of calcareous shale, tends to crumble away between header boards, but is only a minor hazard in the mines studied (fig. 26). As the Anna Shale thickens beneath the Brereton Limestone, the limestone thins and at many places pinches out (fig. 27). The limestone was not observed to fail where more than two feet (>0.6 m) thick, but roof falls are common where the limestone is less than two feet thick, and slips or other deformational structures weakened the cohesiveness.

The "Jamestown Coal interval" at mine A ranges in thickness from a few inches to a little more than a foot (>0.3 m) and includes carbonaceous shale, lenticular limestone, and thin layers of coal. It is an interval of the roof prone to fail without the support of the underlying Brereton Limestone, but where it is underlain by two or more feet (>0.6 m) of limestone, roof stability is satisfactory. In small areas (figs. 24 and 25), all lower units are absent and the "Jamestown Coal interval" directly overlies the Herrin (No. 6) Coal. Major roof falls are abundant in these areas because of the absence of competent strata close to the coal (fig. 28).

The Conant Limestone above the Jamestown Coal interval is the most persistent roof rock member at mine A and maintains a thickness of about one foot throughout the study areas. It is neither thick enough nor strong enough to prevent roof failure where the Brereton Limestone is absent, however. The Conant Limestone is not known to form the immediate roof within the mapped areas.

Overlying the Conant Limestone is the Lawson Shale, a very weak member of the roof sequence at mine A. This member, two to fifteen feet (0.6 to 4.6 m) thick, consists mainly of weak, poorly bedded, mottled, greenish shale with abundant slickensided surfaces. Where the Lawson Shale is thick, two subunits can be distinguished: a lower, moderately firm, dark-gray shale, locally calcareous, and an upper mottled shale. Where the Lawson Shale is exposed by failure of underlying strata, massive falls extending through the Lawson Shale to the base of the Bankston Fork Limestone may

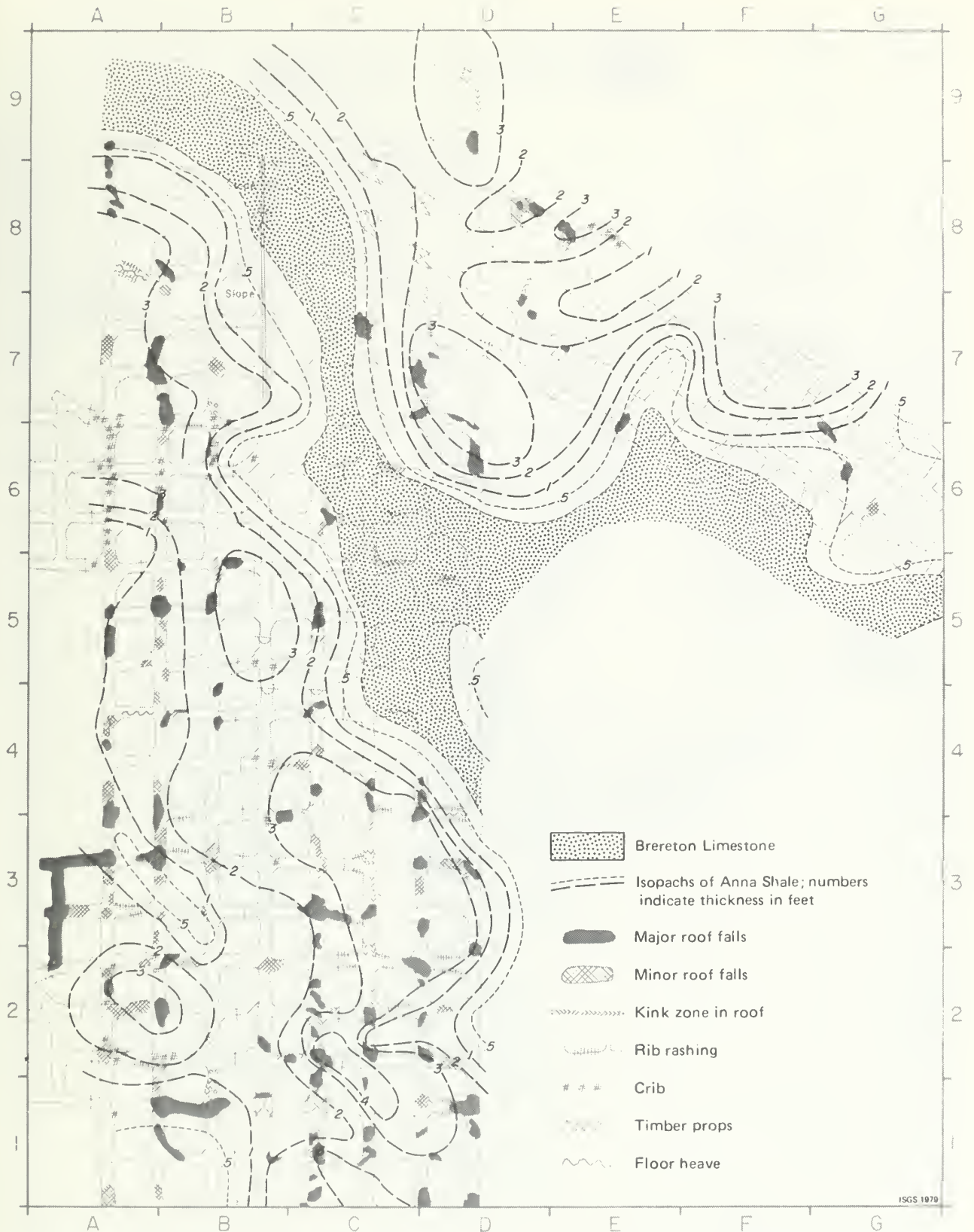


Figure 23. Distribution of roof falls and their relation to the immediate roof strata. No roof falls occur where Brereton Limestone directly overlies the Herrin (No. 6) Coal, although some shallow flaking of "clod" may occur locally. Study area 1, mine A, west-central Illinois. Grid interval is 200 feet (61 m).

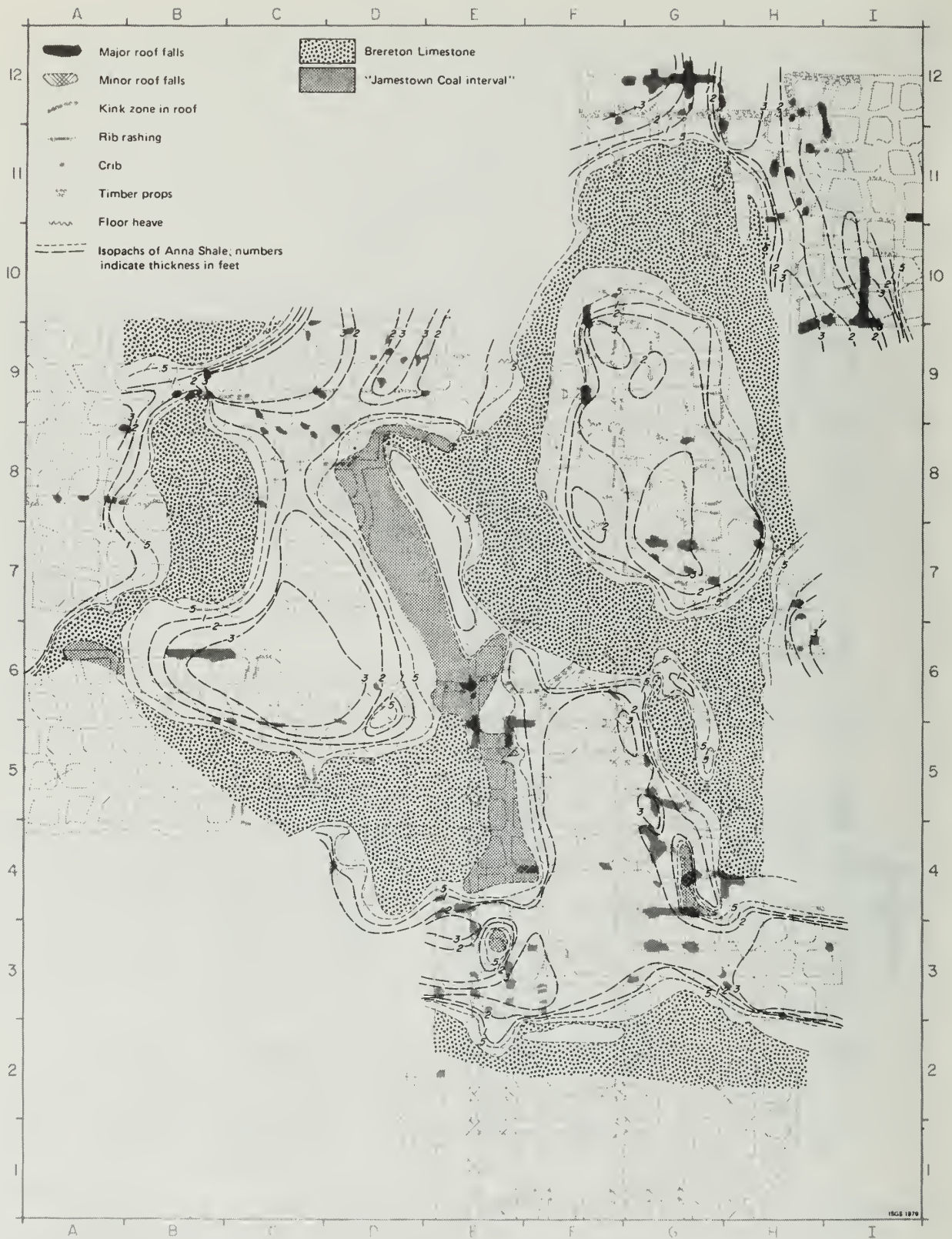


Figure 24. Distribution of roof falls and their relation to the immediate roof strata. No roof falls occur where Brereton Limestone directly overlies the Herrin (No. 6) Coal, although some shallow flaking of "clod" may occur locally. Study area 2, mine A, west-central Illinois. Grid interval is 200 feet (61 m).

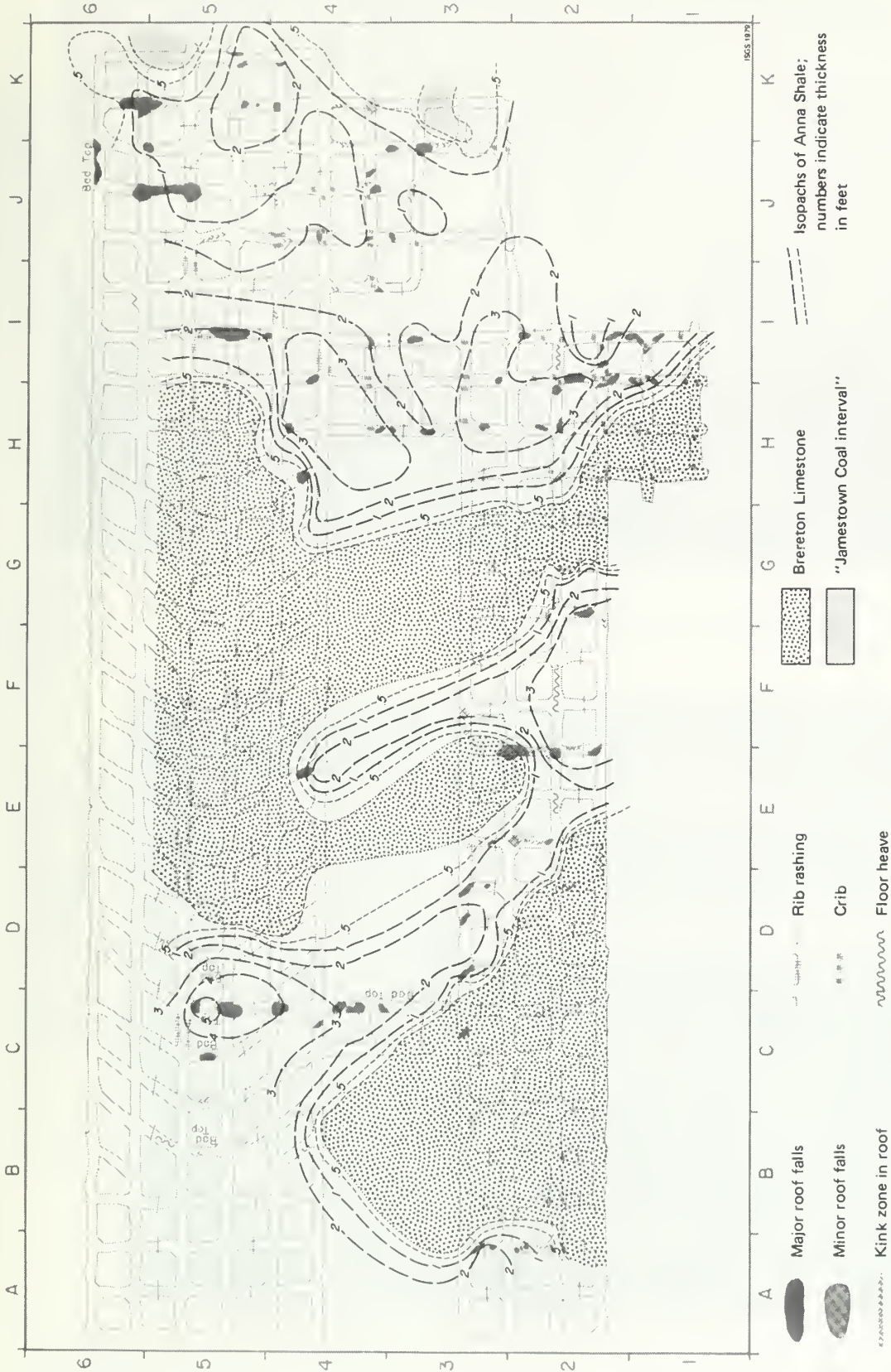
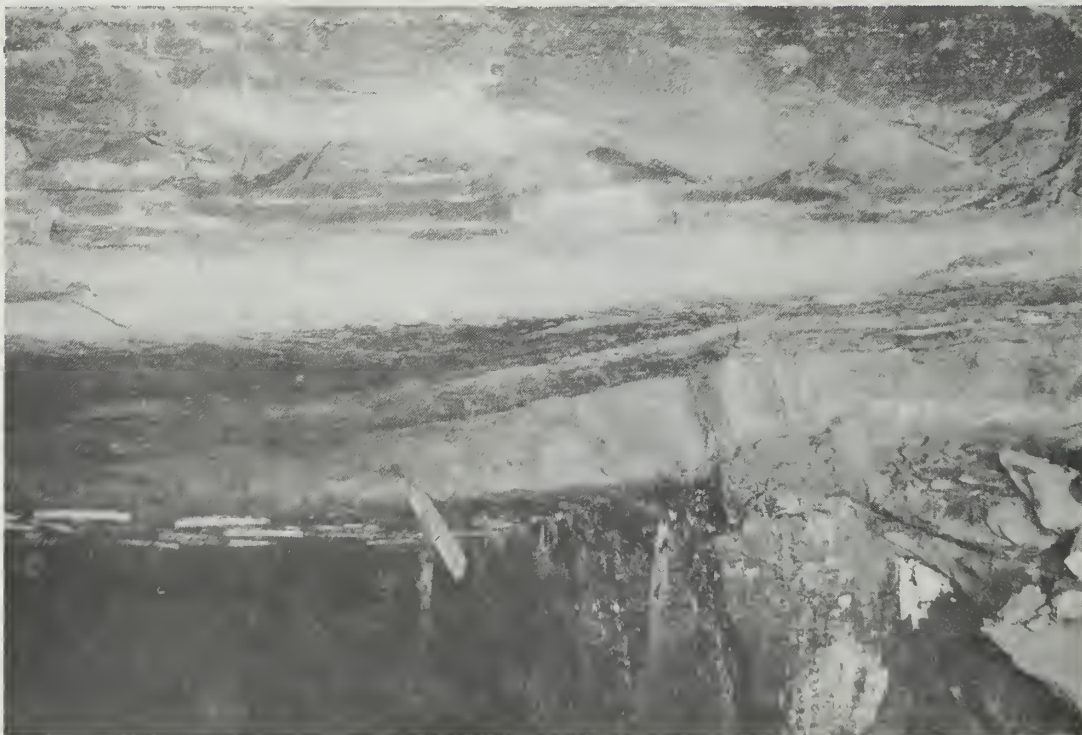


Figure 25. Distribution of roof falls and their relation to the immediate roof strata. No roof falls occur where Brereton Limestone directly overlies the Herrin (No. 6) Coal, although some shallow flaking of "clod" may occur locally. Study area 3, mine A, west-central Illinois. Grid interval is 200 feet (61 m).



Figure 26. Limestone of the Brereton forms stable roof. About the lowest 3 inches (7 to 10 cm) of soft flaky "clod" have fallen, except above the header boards. Location: mine A, west-central Illinois.



Lawson
Shale

Conant
Limestone

"Jamestown
Coal Interval"

Brereton
Limestone

Anna
Shale
.....
Herrin
(No. 6) Coal

Figure 27. Wedging relationship of roof rock layers; both the Anna Shale and the Brereton Limestone pinch out (toward left side of photo). The "Jamestown Coal interval" has thin coal streaks and contributes to bedding separation. The overlying Conant Limestone is too thin to bridge stresses from one pillar to the next. The Lawson Shale is soft and mottled and contains numerous low-angle shear planes and syneresis cracks. Location: mine A, west-central Illinois.

occur (figs. 28, 29). In very few falls the Bankston Fork Limestone also has failed, exposing even higher strata.

The distribution of roof rock bodies at mine A is irregular and variable (figs. 23-25). The Anna Shale is laid out in a patchy pattern of irregular lenses, most of which are several hundred feet in diameter. No preferred orientation of these lenses is apparent. The Brereton Limestone forms the immediate roof in rather narrow belts or troughs between the lenses. Roof rock units below the Bankston Fork Limestone show a reciprocal relationship in thickness; where one unit increases in thickness the other units of the sequence thin (fig. 22). Lowest roof stability occurs where the Anna Shale and the Lawson Shale are thick and the Brereton Limestone is thin.

Deformational structures observed in the black shale-limestone roof type differ considerably from those found in mines with the gray shale roof type. The characteristic structural feature of mine A is the clay dike. Damberger (1970 and 1973) has given a general description of clay dikes in Illinois. This study has yielded many more details that may be found in volume 2. Clay dikes are irregular intrusions of clay from the roof into the coal seam (figs. 30-32). Their inclination varies from roughly vertical to low angle, and they range from a mere film of clay along a minor fault to major "horsebacks" several feet wide. The larger dikes connect with the roof, although they seldom extend more than a foot or so into it. Only the larger dikes penetrate the entire coal seam to the underclay.

The filling of clay dikes consists of soft, usually light-gray clay or silty clay with fragments of coal and roof rocks included in the matrix. The filling was obviously intruded from above, but the filling bears little resemblance to the roof shales because of its alteration; however, the clay mineralogical content of clay dike filling is much closer to that of the roof shale than to that of the underclay (Stepusin, personal communication, 1978).

Directly related to clay dikes are minor faults we have termed *clay-dike faults* (figs. 33, 34). These are usually low-angle normal faults that lack clay filling but show associated secondary deformational features in the coal and roof strata which are typical for clay dikes, specifically:

1. The fault plane is generally shallow in the roof and the top portion of the coal. It steepens downward through the coal and commonly dissipates within the coal in a series of near-vertical extension fractures which are generally mineralized and form an en echelon pattern ("goat beards").
2. "False drag," in which the coal layers curve upwards in the footwall and downwards in the hanging wall, that is, opposite to the direction of normal drag, is abundant (fig. 34). As a result, bedding adjacent to the fault plane tends to be perpendicular to the fault plane.
3. Convergence of coal bedding at the ends of lateral fracture fillings (fig. 33)

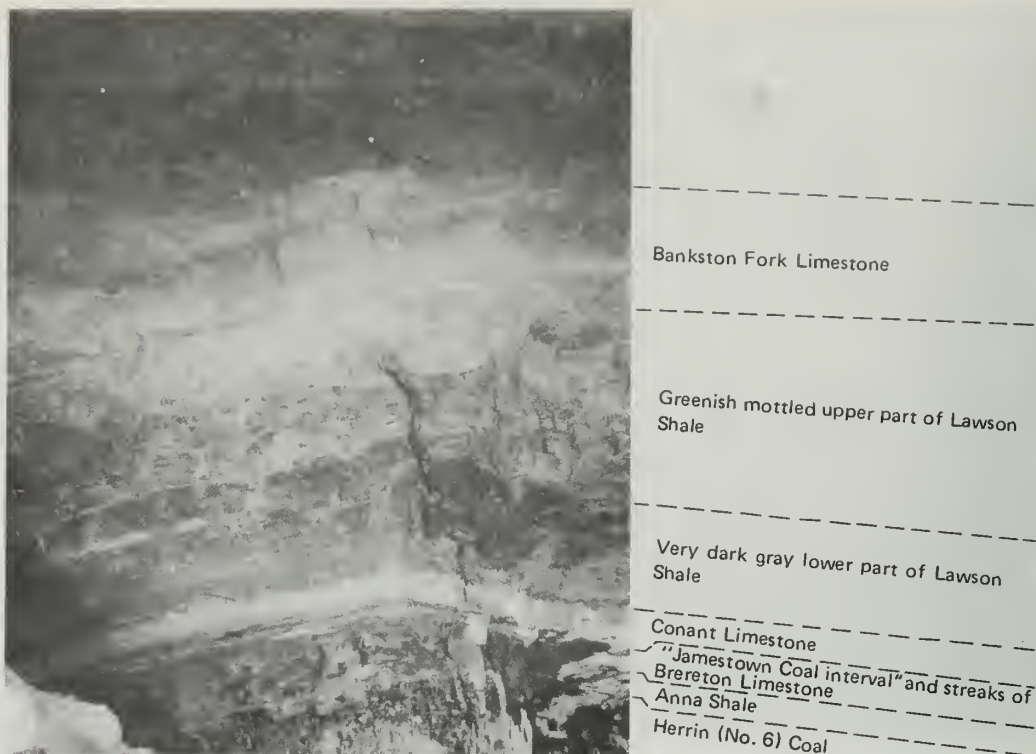


Figure 28. Lawson Shale. Two distinct horizons can be mapped: a lower part that consists of very dark gray to almost black shale that is very calcareous in places and contains concretions (left side of photo) and an upper part that consists of abundantly mottled soft greenish medium-gray shale having numerous syneresis cracks. Location: mine A, west-central Illinois.



Figure 29. Mottled shale with syneresis cracks in greenish medium-gray shale, above very dark gray shale, probably Lawson Shale (with syneresis cracks) above Anna Shale. Note roof bolts hang out bare; the soft shales have fallen because of moisture slaking; in the center of roof fall, even bolt anchors have fallen out. Location: a mine in east-central Illinois.



Figure 30. Clay dike and clay-dike fault in Herrin (No. 6) Coal. Angular fragments of unaltered and altered black shale from the roof and of coal in the clay matrix demonstrate the brittle behavior of the material during deformation. Synthetic and antithetic minor faults are displayed. Note also the plastic behavior of coal, particularly at the end of the small clay intrusion upward, in the upper footwall block. Displayed there is a convergence structure of the coal laminae. Location: mine A, west-central Illinois.



Figure 31. Detail of figure 30.



Figure 32. Complex clay dike in the Herrin (No. 6) Coal. Roof is Brereton Limestone, which is displaced downward to the east. Fusain layer in the center of the coal seam is bent downward east of clay dike, fractured within the clay dike, and offset immediately west of the dike. Note the associated small low-angle clay-dike faults and the numerous extension fractures ("goat beards") and the coal fragments in the clay matrix.

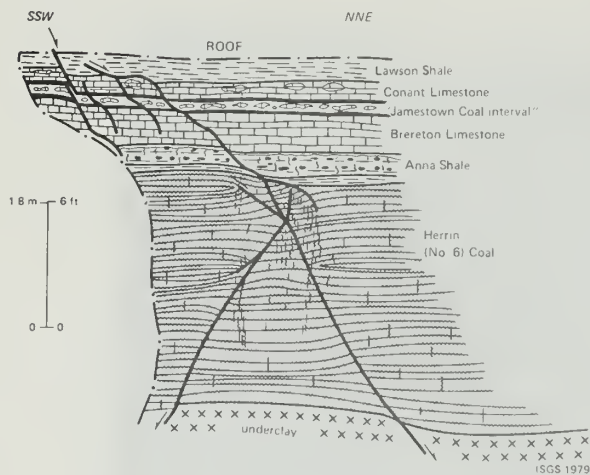


Figure 33. Clay-dike faults dissecting the Herrin (No. 6) Coal and associated rock strata. The faults result not from vertical movements, but mainly from horizontal extension of the strata, as indicated by collapsed grabenlike structures in the upper coal benches and rebound horstlike structures in the underclay and lowest coal benches. Note the convergence of the coal bedding in places, the en echelon extension fractures ("goat beards") and the splitting and downward steepening of the faults in the coal seam. Location: mine A, west-central Illinois.

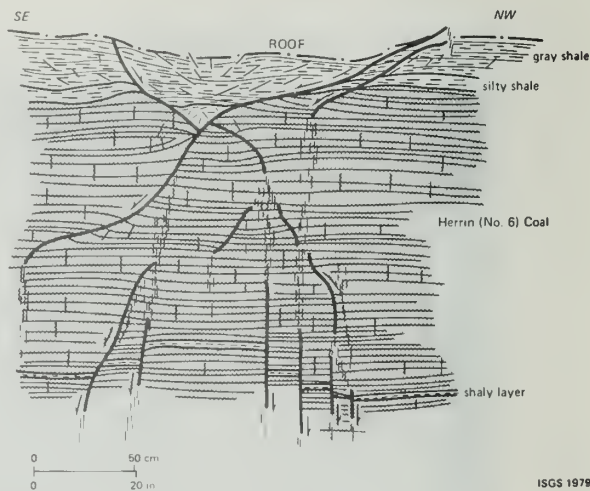


Figure 34. Clay-dike faults forming graben at the top (note the intensely sheared gray shale) and a horst at the bottom of the Herrin (No. 6) Coal. Low-angle normal faults in shales above the coal steepen downward into the coal and dissipate in the form of en echelon extension fractures ("goat beards"). Farther down in the coal seam, faults also form an en echelon pattern and produce a step-faulted horst. Note convergence features of coal beds (upper left area) and false drag. Total deformation is due mainly to horizontal extension with little or no vertical throw of strata. Location: a mine in west-central Illinois.

4. Clay-dike faults usually strike parallel to lithologic boundaries in the immediate roof and dip toward the rock bodies in which they occur.
5. The underclay is mostly buckled upward where clay dikes or the associated faults penetrate the entire coal seam.

The above features indicate that clay dikes and clay-dike faults were formed by lateral extension of the coal seam during diagenesis. In many cases, clay squeezed in along the opening fissures, forming clay dikes. In other places where the amount of extension was insufficient, no clay entered, but slickensided clay-dike faults developed.

Clay dikes themselves rarely cause major roof falls because they seldom extend more than a foot or two into the roof. Larger clay-dike faults, however, can seriously affect roof stability, particularly where two or more intersect above the coal seam. The largest clay-dike faults found offset the coal as much as 18 feet (5.5 m) and displace strata through the Bankston Fork Limestone. Major roof falls result from these faults and alteration in the mining plan is necessary. More details are presented on this topic in the next section.

As in mines B and C, joints at mine A contribute only to a few large roof falls, but slabbing between joint planes is a common hazard. Joints are common in conjugate vertical sets in an orientation N 55° to 80° E and N 145° to 160° E with a spacing of about three to ten per foot.

Joints normally penetrate only the lower, fissile portion of the Anna Shale and result in only minor slabbing of that unit. All major roof falls at mine A are caused by absence of competent strata (Brereton Limestone) in the roof sequence, especially where clay-dike faults are present.

MAPS AND EXPLANATION OF THE GEOLOGY IN SELECTED STUDY AREAS

Seven study areas in three mines were mapped in detail, and a wide variety of geologic maps were prepared. Only the compilation maps are presented here (figs. 13-16, 23-25, and 35-37). For a more complete suite of maps, the reader is directed to volume 2 of Krausse et al., 1979. Similarly, only three examples of regional computer-generated maps (figs. 38-40) have been included here. Additional ones are included in volume 2 of the complete report. Figures 39 and 40 present a generalized picture of the thicknesses and structures. Because of the wide spacing of the datum points (an average data density of less than 1 datum point per square mile), the features of the maps are interpretive and do not show true thickness. They are, however, useful as guides for thickness trends and statistical variability of the rock units in different areas of the state. The maps of study areas 1 to 3 at mine A (figs. 23-25, 35-37) display similar lithologic, structural, and roof-stability patterns. The relationship between roof lithology and roof stability is apparent. No significant roof falls occur in areas of immediate limestone roof, but numerous falls have been spotted in regions of Anna Shale or "Jamestown Coal interval" roof. Fewer falls occur adjacent to immediate limestone roof areas than farther away from them, because adjacent to limestone roof areas the Brereton Limestone is present above the Anna Shale. Limestone tends to thin and pinch out as the Anna Shale thickens.

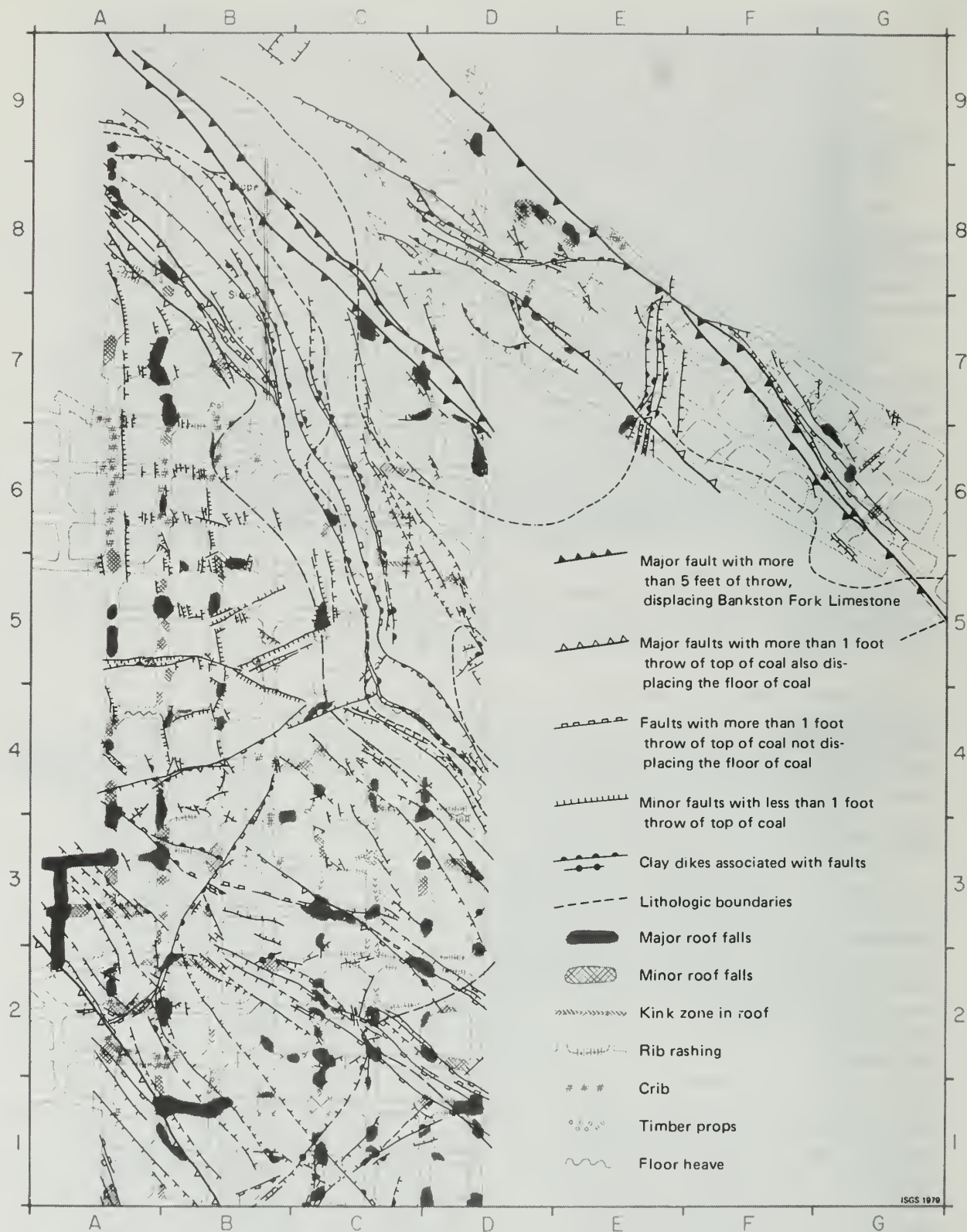


Figure 35. Distribution of clay-dike faults and clay dikes in the Herrin (No. 6) Coal and its immediate roof strata and of roof falls and other induced instabilities in study area 1, mine A. The occurrence of roof falls is a function of two geologic variables: (1) lithologic distribution and pattern of roof rocks and (2) structural setting and fault pattern. Roof falls are abundant along faults and slips; however, there appears to be a greater affinity of roof falls to the lithology than to faults. Grid interval is 200 feet (61 m). (See also appendix figure A.)

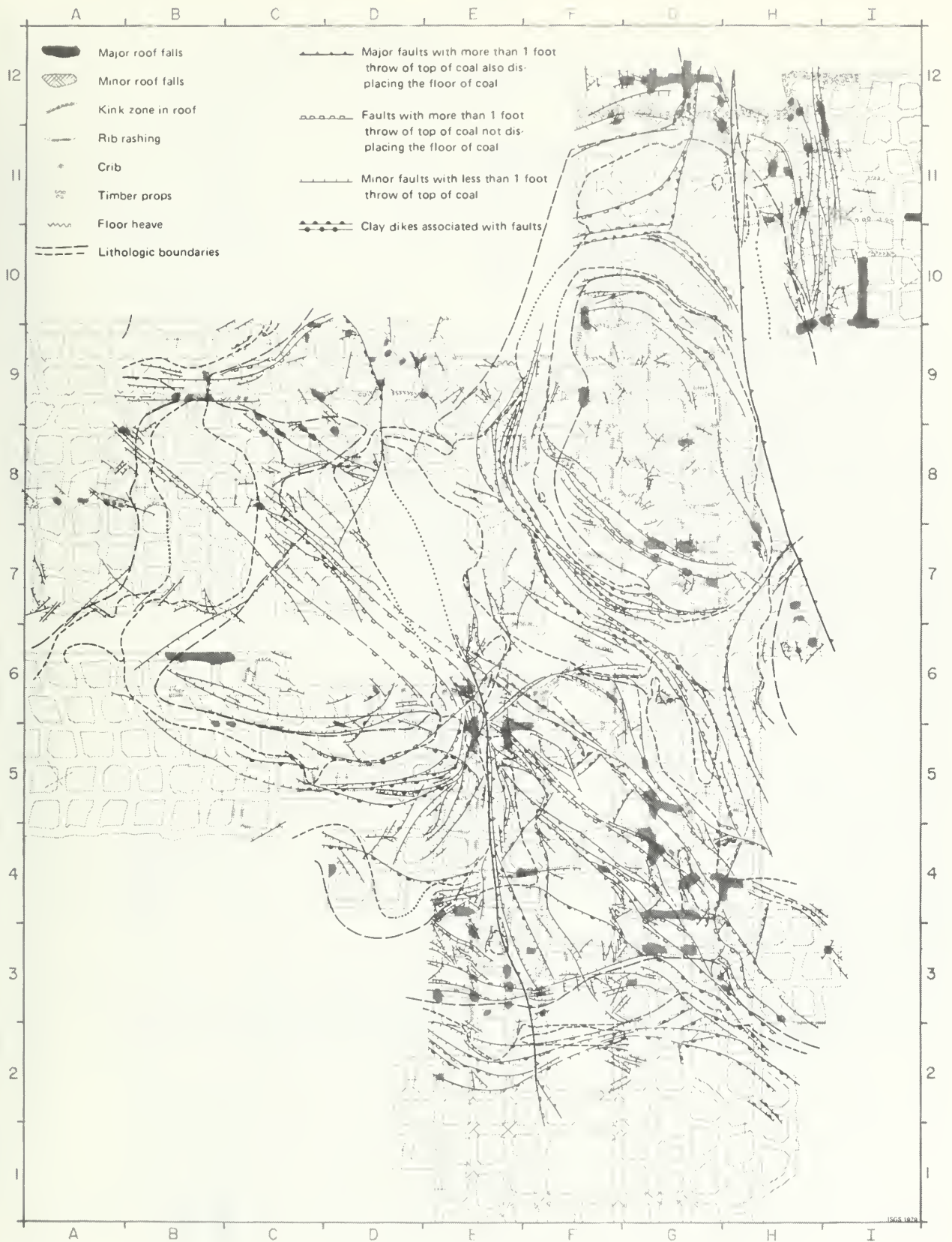


Figure 36. Distribution of clay-dike faults and clay dikes in the Herrin (No. 6) Coal and its immediate roof strata and of roof falls and other induced instabilities in study area 2, mine A. The occurrence of roof falls is a function of two geologic variables: (1) lithologic distribution and pattern of roof rocks and (2) structural setting and fault pattern. Roof falls are abundant along faults and slips; however, there appears to be a greater affinity of roof falls to the lithology than to faults. Grid interval is 200 feet (61 m).

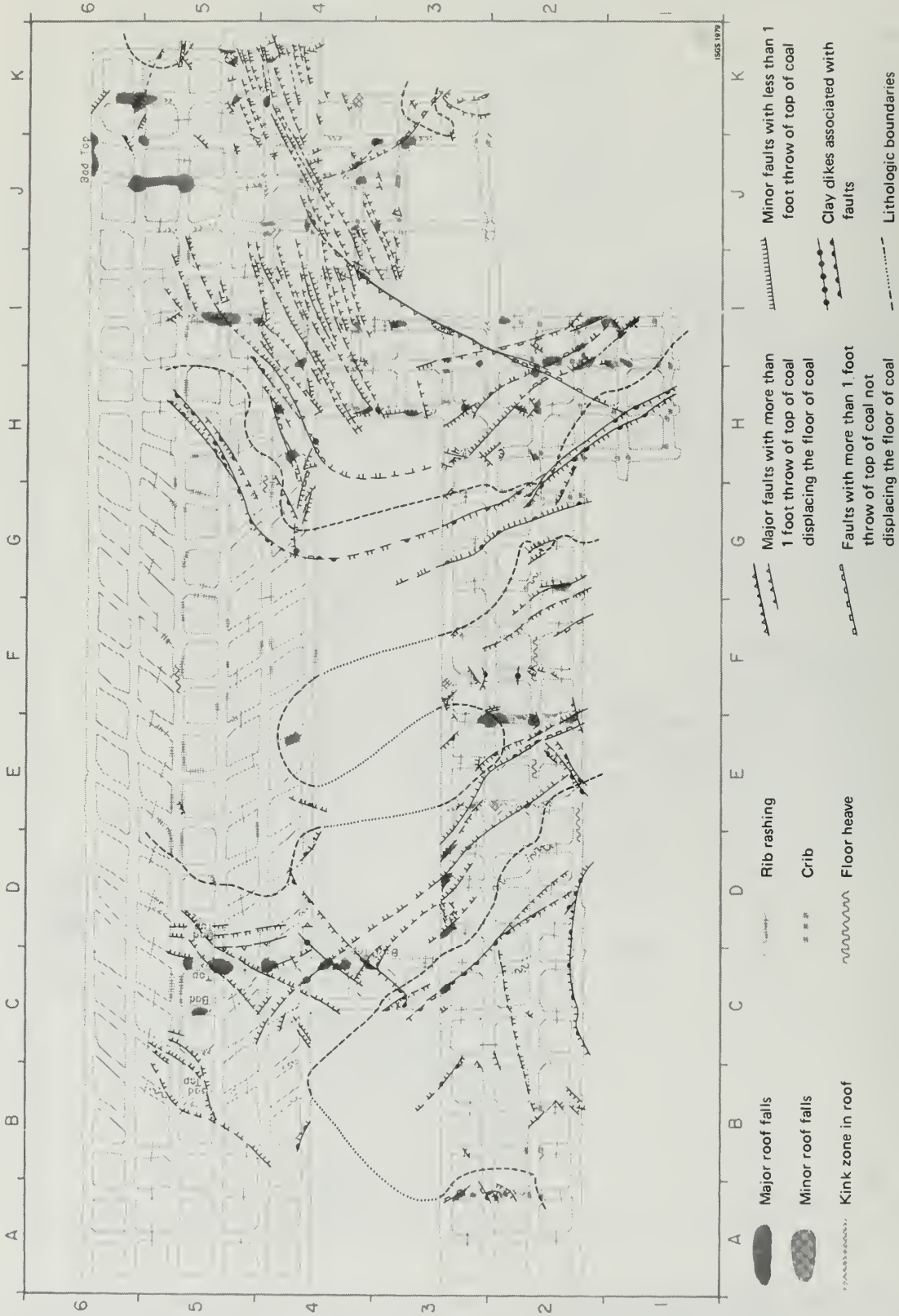
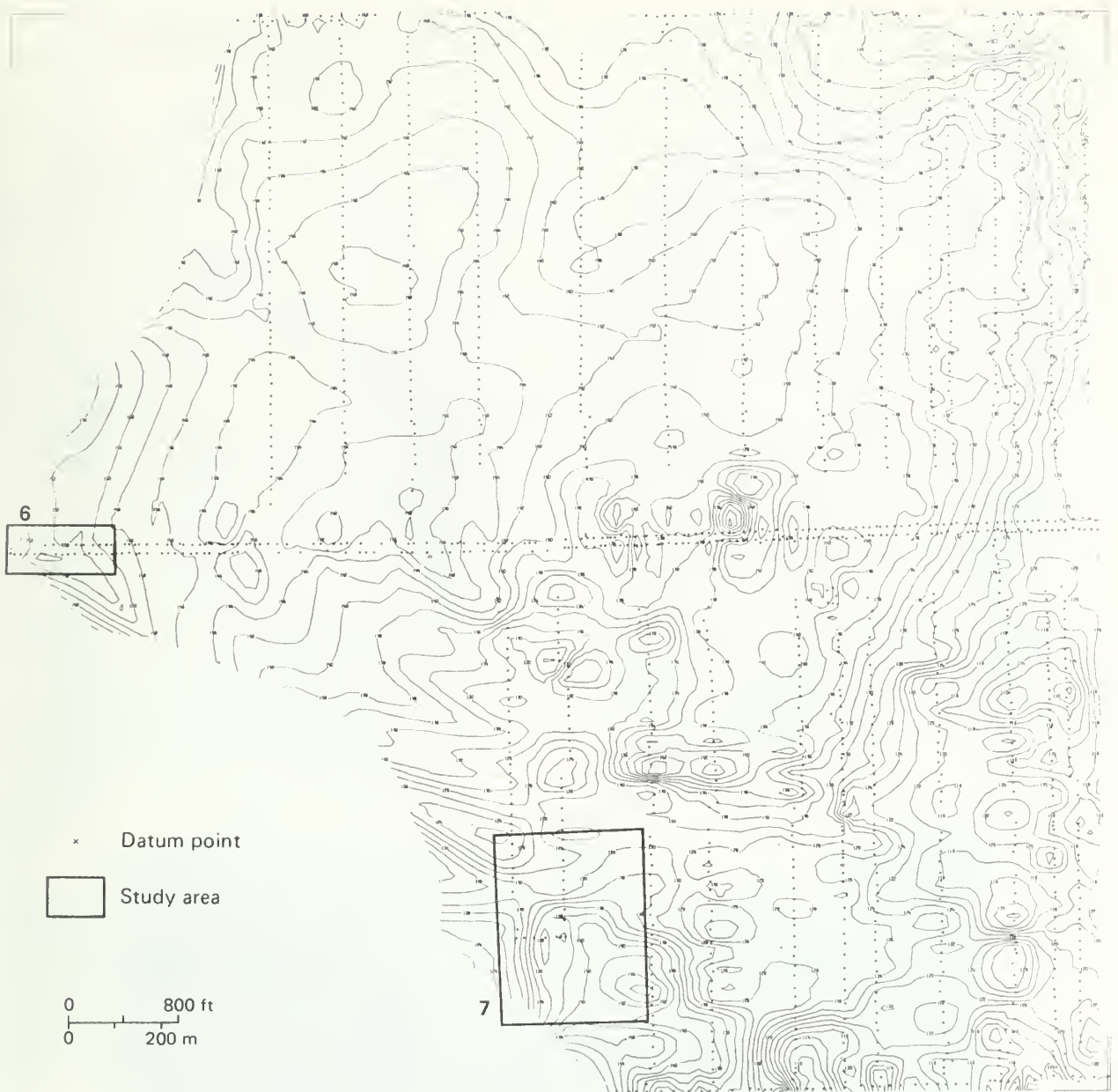


Figure 37. Distribution of clay-dike faults and roof falls in the Herrin (No. 6) Coal and its immediate roof strata and of roof falls and other induced instabilities in study area 3, mine A. The occurrence of roof falls is a function of two geologic variables: (1) lithologic distribution and pattern of roof rocks and (2) structural setting and fault pattern. Roof falls are abundant along faults and slips; however, there appears to be a greater affinity of roof falls to the lithology than to faults. Grid interval is 200 feet (61 m).



ISGS 1979

Figure 38. Computer-generated map of the elevation of the top of the Herrin (No. 6) Coal at mine C, study areas 6 and 7. Structural anomalies of the top of the coal reflect anomalies in the roof strata of mainly laminated siltstone and sandstone, which locally impose severe problems for roof control. Contour interval: two feet; grid size: 100 feet.

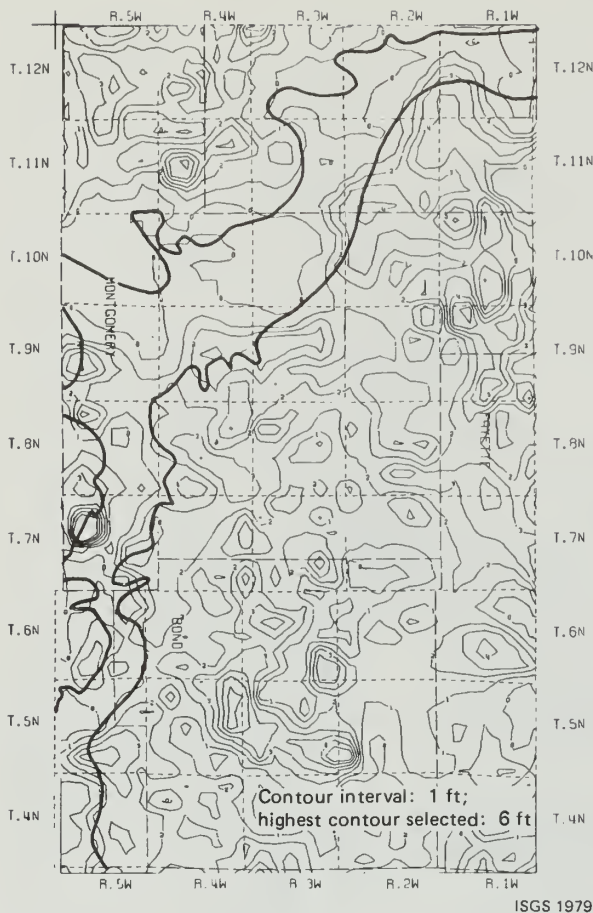


Figure 39. Thickness trends of the Anna Shale Member in Bond and Montgomery Counties. The isopach map shows the patchy and very lenticular occurrence of the Anna Shale just as it was observed for the "Quality Circle" area and for the rest of southern and southwestern Illinois. The Anna Shale is generally less than four feet (1.2 m) thick but may locally exceed six feet (1.8 m) in thickness. Neither a regular distribution pattern nor a trend in Anna Shale thickness is visible. The lenticular pattern, however, has been observed in study areas 1, 2, and 3.

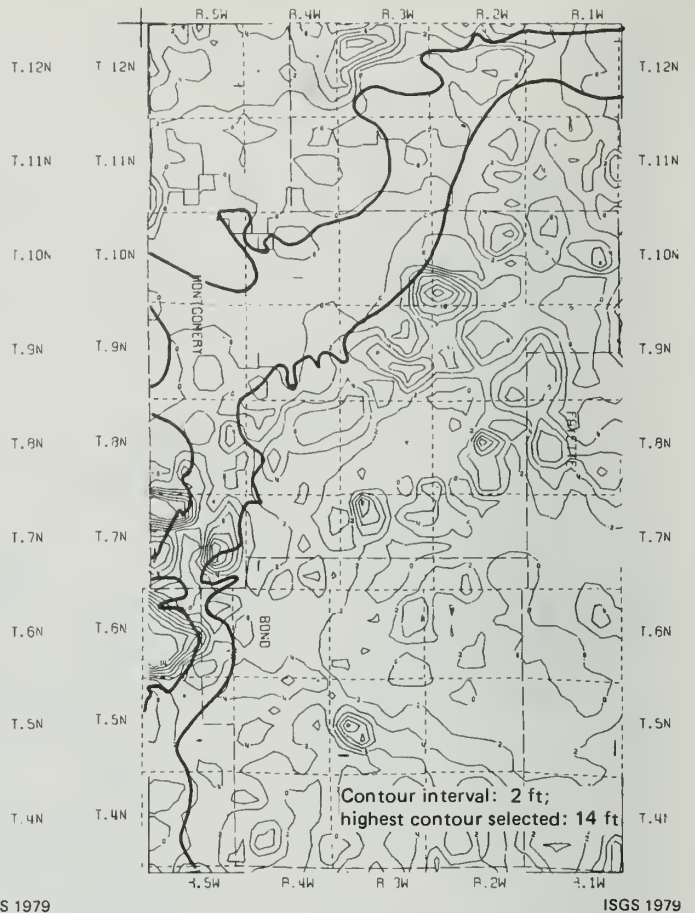


Figure 40. Thickness trends of the Brereton Limestone Member in Bond and Montgomery Counties. The Brereton Limestone occurs in lenticular patches. The isopach map at first appears similar to the previous one of the Anna Shale, but in many places a reciprocal relationship between the thickness of the Brereton Limestone and the Anna Shale is shown, just as it has been found in study areas 1, 2, and 3.

Figures 39 and 40. Size of area—1,620 miles² (3,226 km²); Average distance between points—1.6 miles (2.58 km); Grid size—5,000 feet (1,525.0 m); Maximum search distance—50,000 feet (15,240.0 m); Number of data points—817 (about 250 of these were outside the map area). Areas with > 2 miles between data points: 7N-1W, 6N-1W, 5N-1W, 4N-1W, 11N-4W, 11N-3W, 10N-5W. The heavy outline of the areas of thin, split or missing coal was hand drawn independently from these maps using a greater data point density.

The relationship of faults to lithology is complex, but is well shown on the maps. Three general classes of faults can be defined:

1. Major clay-dike faults that have a displacement of a seam's thickness or more (directional dip indicated on map by solid triangle). A set of these faults is shown in the northern part of the area in figure 35. These large faults tend to form an en echelon pattern along the strike and cut across roof lithologic boundaries. A tectonic origin for these faults cannot be completely ruled out, but certain features, notably the false drag and the shallow dip angle (fig. 41) strongly suggest that they formed while sediments were not yet completely consolidated. Their distribution and orientation might be controlled by larger-scale depositional or compactional geologic settings not reflected in the immediate roof rock, and thus in the maps.
2. Clay dikes and clay-dike faults displacing the top of the coal seam more than one foot and extending into the underclay. These are shown by open-square dip symbols. Like the major faults, many of them tend to follow rather straight courses without regard for lithologic boundaries and are formed during diagenesis in response to large-scale patterns not directly reflected in the immediate roof (fig. 36, diagonally through center of map).
3. Minor clay dikes and clay-dike faults displacing the roof generally by less than one foot, but not displacing the floor of the coal seam, are shown on the maps by hachured lines. These faults show a strong parallelism to roof lithologic boundaries. Most faults of this type dip toward the center of the lithologic body within which they occur. Clay

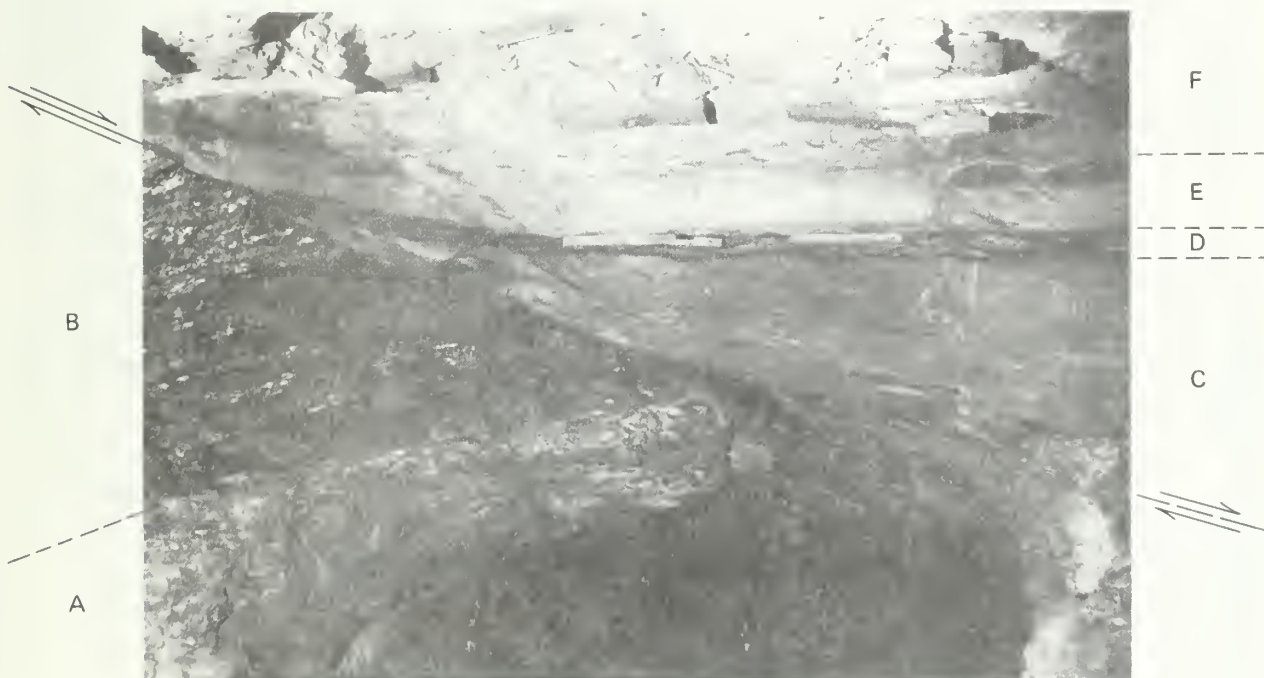


Figure 41. Clay-dike fault. Low-angle normal fault (dip angle 35° to 50°) with more than twelve feet (3.6 m) of throw (on figure 35, area A/9 to D/ 7). Shales, calcareous strata, and lower portion of Herrin (No. 6) Coal show normal drag, whereas upper portion of the coal displays false drag. Strata from the underclay of Springfield (No. 5) Coal up to the Bankston Fork Limestone are truncated. Photo shows A—underclay; B—Herrin (No. 6) Coal; C—Brereton Limestone; D—"James-town Coal interval"; E—Conant Limestone; and F—Lawson Shale. Location: study area 1, mine A, west-central Illinois.

dikes are most often found under limestone roofs, but clay-dike faults are just as abundant under shale roofs as under limestone roofs. The pattern observed strongly suggests that the minor clay dikes and faults formed during sediment compaction and were influenced or generated by differential compaction. As the volume of coal and of the associated rock bodies changed during compaction, extension fractures and slip surfaces developed to adjust for differences in compaction rates.

The maps of study area 4, mine B, show the dominantly dark-gray Energy Shale roof (fig. 13). Medium-gray shale roof (stippled pattern on map) forms a complex, digitate pattern. Rolls are clearly confined to medium-gray shale and show rough parallelism to lithologic boundaries; however, roof failure occurs mainly along north-south headings and apparently is independent of structure and lithology. As stated previously, this north-south orientation of roof falls and kink zones is not fully explained. It may be related to the north-south-trending Rend Lake Fault System, which passes west of the study area.

In study area 5, mine B, rolls are again confined to medium-gray shale roof areas. The map (fig. 14) shows a strong tendency of the rolls to parallel lithologic boundaries, but the dominant feature controlling roof stability is the shear body, outlined by the bold dashed line in figure 15. The spacing of roof falls in the shear body area is much denser than in any other area mapped for this study. Were it not for extensive cribbing and use of rail bars for roof support, many large falls undoubtedly would have occurred.

As the map of study area 6, mine C (fig. 42) indicates, the most severe roof falls and rib rashing occur where the planar-bedded sandstone lies close to or directly on top of the coal seam. The line of demarcation between wet and dry roof also relates to the height of sandstone above the coal. In the northeastern corner of the map, where 20 feet or more of medium-gray shale intervenes between coal and sandstone, roof and ribs are dry and stable.

A similar pattern is seen in study area 7, mine C (fig. 16). Additional mining problems resulted from steep inclination of the coal and from large sandstone rolls, which generally strike southeastward, parallel with the sandstone-shale roof boundary. The largest roll, marked on the map as the "mega-roll," necessitated alteration of the mining plan and grading entries through rock, as face equipment could not follow the steep inclination of the coal.

The overall relationship between study areas 6 and 7 is shown on the computer-generated map of the top of the coal (fig. 38). In most of the map area, the coal is roughly flat-lying and has small circular domes and depressions, but in the vicinity of areas 6 and 7, contour lines trend northwest to southeast, parallel with the roof lithologic and structural trend. This parallelism is evidence that present structural features may still reflect ancient topographic features and thus that deposition of roof sediments may have been influenced by coal topography.

Two small-scale regional maps (figs. 39 and 40) are presented as examples of computer-generated mapping. Figure 39 is a map of the thickness of the Anna Shale in Bond and Montgomery Counties. The patchy, lenticular distribution of Anna Shale is reflected on the regional scale and has been mapped similarly in mine A on a larger scale. Figure 40 shows the

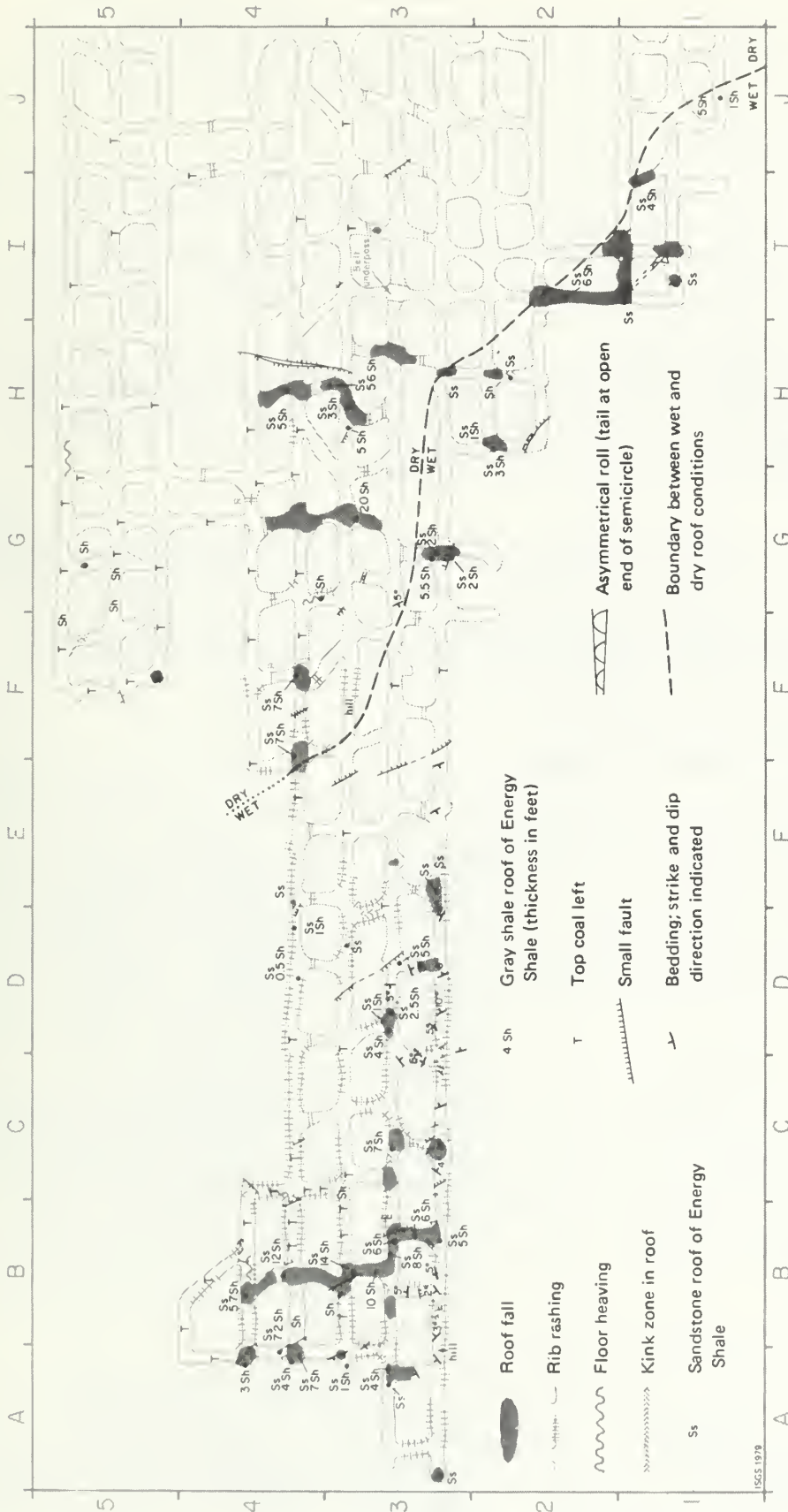


Figure 42. Lithology and minor fault structures of the Herrin (No. 6) Coal and its immediate roof strata and distribution of roof falls and other induced instabilities in study area 6, mine C. Grid interval is 200 feet (61 m).

thickness of the Brereton Limestone for the same area. Although no clear pattern of preferred lithologic distribution trends emerges, a general reciprocal relationship between the thicknesses of the Anna Shale and the Brereton Limestone can be observed by close comparison of the two maps.

OBSERVATIONS AND DISCUSSION OF ROOF FAILURE TRENDS

An attempt was made to quantify the observations made during in-mine mapping. A series of tables correlating roof failure with roof lithology and structures in the various study areas was prepared. As expected, the tables confirm the inferences derived from a study of the maps. For presentation of tables and detailed discussion, the reader is directed to volume 2.

The best roof conditions under the black shale-limestone roof type are found where thick limestone forms the immediate roof. Black shale containing clay dikes and clay-dikes faults is less stable than black shale without these structural interruptions. Roof stability increases in direct proportion to thickness of the limestone overlying the black shale.

In study areas with the gray shale roof type, undisturbed medium-gray shale is the most stable roof rock, followed by dark-gray shale, with planar-bedded siltstone and sandstone the least stable. Again, presence of slips and rolls decreases roof stability, but the highest percentage of fallen intersections was recorded within the shear body. Wet roof is considerably more prone to failure than dry roof in study areas 6 and 7.

MATERIAL PROPERTIES AND DESIGN CRITERIA

Coal, floor, and roof materials vary widely in relative stiffness (Young's modulus) and strength (unconfined compressive strength), as shown in figure 43.

Similarly, test values for roof-bolt pullout vary greatly; a range of 6,000 to 12,000 pounds pullout force was recorded at one mine. In general, massive rocks such as limestone or unlaminated siltstone will hold bolts better than well-bedded rocks where bedding-plane separation can be expected, such as in the planar-bedded sandstone of mine C. The laminated coarse clastic rocks also are lower in compressive strength than nonlaminated, massive shale or siltstone. Another important factor is moisture content; e.g., shales high in moisture generally are less stable in mine openings than shales low in moisture.

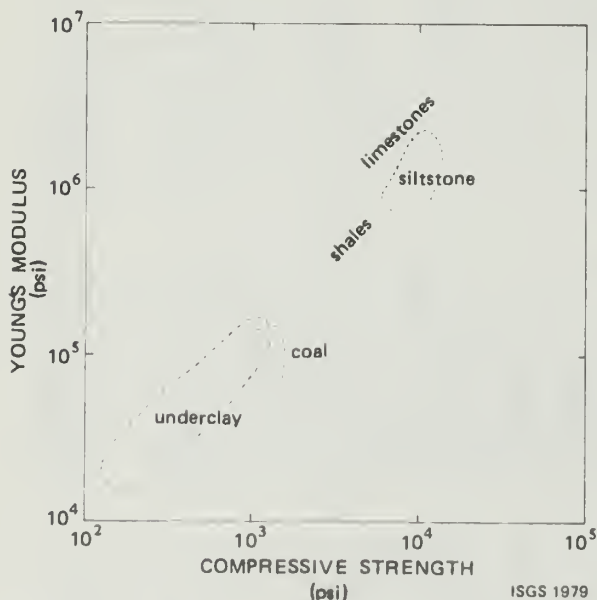


Figure 43. Generalized rock strength of roof-pillar-floor materials in Illinois, based on intact core samples.

Petrographic factors and the rock fabric have a bearing on roof stability, but their effect is generally overwhelmed by structural discontinuities and disturbances such as bedding separation, fractures, faults, and rolls:

1. Rocks that contain relatively little clay and are cemented with calcite, dolomite, siderite, or silica generally make stable roof (e.g., siltstone and massive sandstone).
2. Black shale, despite its fissility, is also a relatively stable roof material because the organic matter in the shale is chiefly in a colloidal stage and acts as binder for the particles, and the clay minerals are oriented parallel to bedding.
3. Argillaceous siltstones, mudstones, poorly bedded shales, and very argillaceous limestones cause roof instability because of the abundance of slickensides and syneresis cracks, and because of their permeability along fractures and affinity for water.
4. Claystones result in the most unstable roof because of their high content of randomly oriented clay minerals, great affinity for water, and numerous slickensides and syneresis cracks.

CONCLUSIONS

Geologic interpretations

The lithologic distribution patterns in both gray shale and black shale-limestone roof types are much more intricate, irregular, and patchy than previously suspected. Exploratory drilling can provide coal companies with only a general idea of roof conditions in the area, but cannot be used to map local, yet relevant, lithologic patterns tens to a few hundred feet in size. It is precisely these local irregularities which have the greatest influence on roof stability.

Present-day distribution of roof rock reflects conditions that existed in the coal-forming swamp during and immediately after peat accumulation. In the vast, almost level, swamps, minor local variations in topography and compaction of the plant material probably had a profound effect on local sediment deposition, regardless of whether conditions were marine (black shale-limestone), nonmarine (gray shale), or transitional (fig. 44).

In any depositional environment, small depressions in the swamp surface would have been the first sites of deposition. The sediment might have been dark-gray mud in the nonmarine environment or black mud in the marine situation. These sediments, which became the dark-gray facies of the older Energy Shale and the younger Anna Shale, respectively, both have much in common. Both are fine grained, finely laminated, and contain a high content of carbonaceous matter; these conditions indicate deposition in quiet anoxic water.

As the dark sediments accumulated, their weight caused the underlying spongy peat to compress, deepening and widening the depression and allowing continued sedimentation up to a certain compactional stage of the peat, until a more regional change in depositional environment, such as transgression or regression of the sea, occurred to change the nature of the sediment being deposited. Medium-gray mud began to accumulate above the dark-gray shale in nonmarine areas, and the Brereton Limestone was deposited

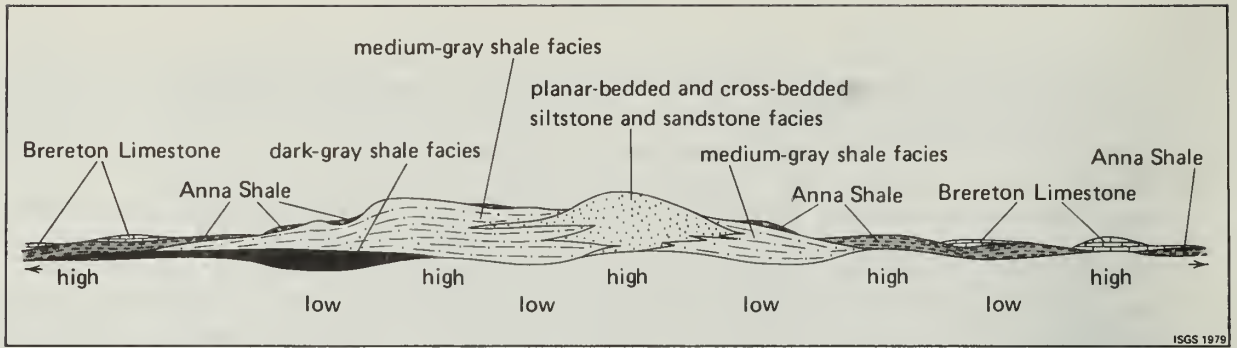


Figure 44. Diagram of the common relationship between the first two units of roof rock immediately above the Herrin (No. 6) Coal and their effect on topography of the surface of the coal. (Vertical scale is greatly exaggerated.)

above the Anna Shale in marine areas. Even younger sediments were deposited over the older sediments or on top of the still uncovered peat.

During all this time, the coal-forming material continued to compact differentially depending on the amount of previous compaction and the additional weight of the accumulating overburden. Eventually, early compaction decreased as the peat approached compressibility limits in the areas of longest and thickest sedimentation. Sedimentation slowed in these areas, whereas adjacent areas, where the peat was still compactable, continued to receive sediment. Thus, an inverse thickness relationship could develop, e.g., the areas with thickest Anna Shale would receive the thinnest limestone, and vice versa.

The primary depositional shape of the rock bodies was deformed locally by various processes, such as loading, compaction, or gravity sliding. The most spectacular example is the shear body at mine B. Smaller-scale soft-sediment flow and slump is indicated by folded laminations near rolls in gray shale and sandstone. In the black shale-limestone roof type, less direct evidence of lateral flow and folding has been found, but lateral adjustment also occurred in shale units during compaction, as shown by secondary thinning of beds.

Practically all the deformational features mapped during this study can be attributed to soft-sediment deformation in a broad sense, that is, they were formed before the sediments were fully compacted and lithified. Sediments vary widely in their original mechanical and chemical properties and in their rates of lithification. Some rock units, notably coal, may have reacted to overburden stress by brittle deformation, while other lithologies reacted by ductile flow or plastic deformation. In some cases, plastic and brittle deformation have occurred side-by-side in the same coal or rock unit.

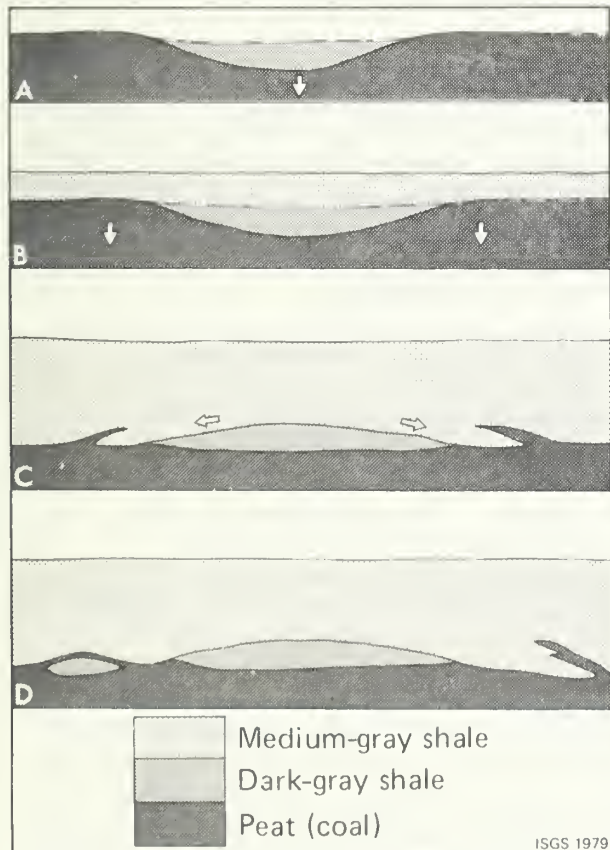
The different deformational elements in the gray shale roof type in contrast to those in the black shale-limestone roof type probably relate to different physical properties of the original sediments. Depositional environment, rate of accumulation, and rate of compaction certainly also have a major influence on deformation. As yet, however,

we cannot show what property of medium-gray shale is conducive to roll formation, or what properties of the black shale-limestone roof lead to formation of clay dikes.

For the area of mine B, Edwards (1976) has suggested a hypothesis on roll formation, which, however, is not easily applicable to roll formation in other areas, as, for instance, that of mine C: the first stage is deposition of dark-gray shale in depressions in the peat swamp (fig. 45a). Next, medium-gray shale is laid down as a blanket deposit over the peat and dark-gray shale (b). In the third stage, compaction of the peat creates an inversion of topography, leaving dark-gray shale lenses as highs (c) down which medium-gray shale could slump. Masses of gray shale could then intrude into irregularities in the peat, lifting up the top layers to form the "rider." The final result is that lenses of shale remain within the coal, with coal "riders" above.

As previously noted, the shear body in study area 5 is interpreted as a gravitational sliding. It is younger than rolls, as shown by truncation of the tops of rolls by the shear body (fig. 19). The triggering event might have been an earth tremor, or simply pure overburden stress initiating the slide along a very gently sloping surface.

Clay dikes and clay-dike faults are the dominant deformational features of the black shale-limestone roof type. Like rolls, they are diagenetic deformational features, formed under sediment cover. They apparently devel-



oped after the first coalification stage of the plant material, but prior to ordinary cleat formation, as coal cleats are not deformed in the vicinity of clay dikes. The clay definitely was intruded from above. The structure of faults, dikes, and associated features indicates that lateral extension, rather than vertical movement, predominated. The stretching and fracturing of the coal seam might have been a gradual process during diagenesis. A sudden reaction and relief of overburden loading may have caused the fracturing of the coal and formation of clay dikes, or, as Damberger (1970, 1973) has suggested, earthquakes may have been responsible for rupturing the coal and intrusion of the clay.

Figure 45. Interpretive sequence of roll formation. (From Edwards, 1976.)

Recommendations

This investigation has shown that roof stability is closely related to the geologic setting and patterns that are highly variable, intricate, and difficult to predict in advance of mining. Roof conditions may change abruptly within a distance of less than 100 feet (30 m). In one entry the roof may remain stable for the life of the mine with a minimum of artificial support, while the adjacent entry may collapse immediately unless additional support has been installed. Therefore, much greater flexibility in roof control planning is needed.

In gray shale roof areas, rolls can be a major roof hazard. Roof bolts always should be anchored well above the coal "rider" so that separation cannot occur along this plane of weakness. For small rolls it might be advantageous to bring down the shale lens below the "rider" before bolting. Very large rolls may require timbers or cribs in addition to roof bolts.

Planar-bedded siltstone and sandstone also make the mine roof difficult to control. Where roof bolts of equal length are used, the siltstone strata tend to separate at the next bedding plane in or above the bolt anchors. In this case roof control might be improved by using bolts of several different lengths to reduce the splitting effect anchors may impose and to distribute the load over several bedding surfaces. Resin bolts could help further by binding rock layers together along the entire length of the bolt. In many cases, however, bolts would have to be supplemented by cribs or timbers.

A shear body like that encountered in study area 5 presents a real challenge in roof control. Mechanical bolts are of little value, as their anchors will not take sufficient hold in densely sheared rock. Use of resin bolts of different lengths would probably be an improvement, but a comprehensive roof control program would demand additional support by cribs, 3-piece sets, and rail bars set into the ribs. This additional support should be placed as soon as the sheared roof condition is recognized.

In black shale-limestone roof areas, the Brereton Limestone as immediate roof requires the minimum artificial support. In mined-out areas, entries with limestone roof have remained stable for more than 20 years without any artificial support. In areas of black shale, roof bolts should be anchored at least one foot (0.3 m) into the first limestone bed more than two feet (>0.6 m) thick. The position of the limestone can be determined by drilling test holes with the bolting machine. Where no limestone more than two feet thick exists within an interval of 10 to 15 feet (3 to 4.5 m) above the top of the coal, timbers may be needed for long-term support.

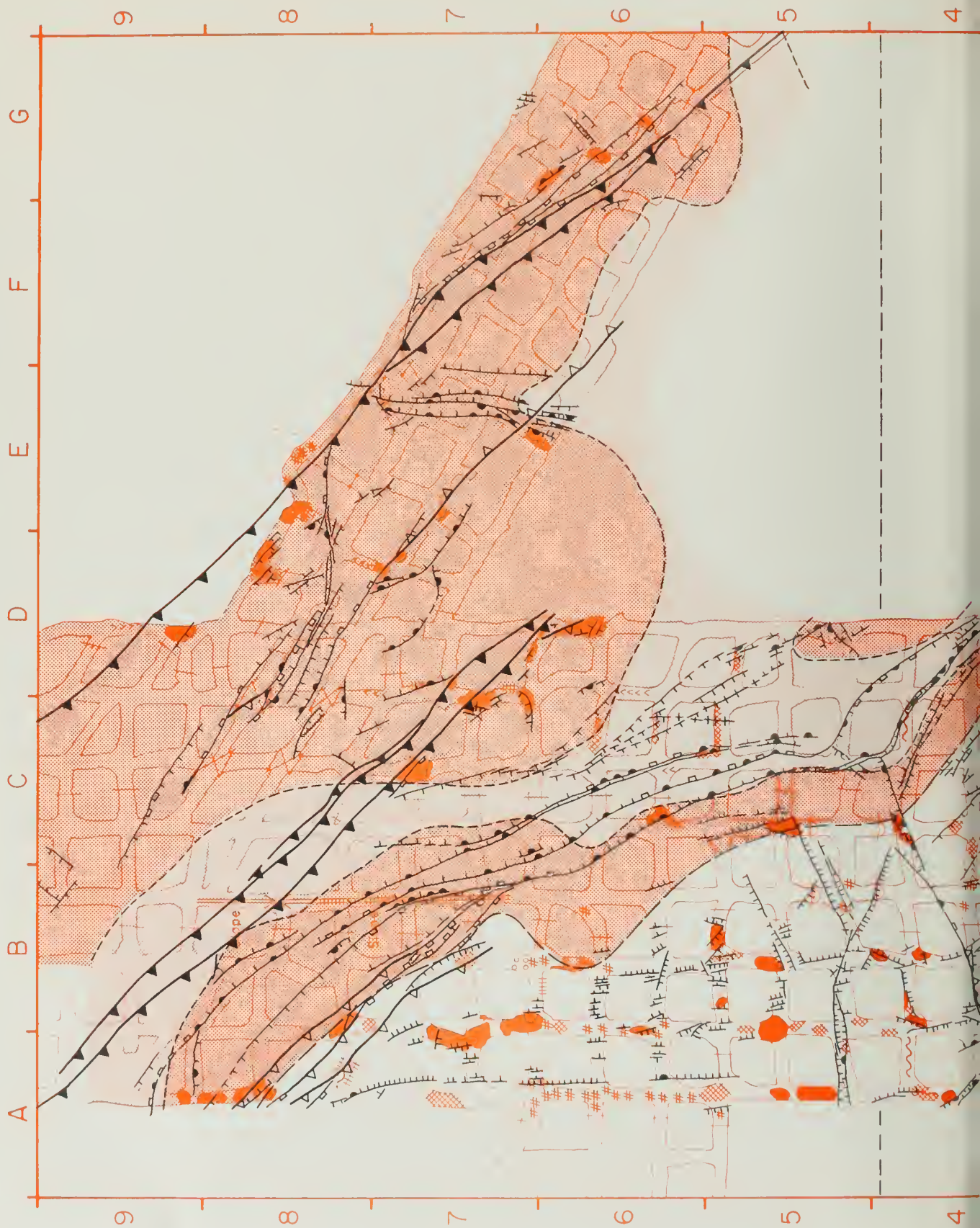
Clay-dike faults are generally too variable in strike and continuity to allow major alterations of the mining plan to avoid them; however, local changes in pillar layout can be made to avoid having large faults run parallel to mine openings over a long distance. Major tectonic faults and fracture zones, and kink zones such as the north-south set encountered in study area 4, are more predictable. Frequently roof control may be improved by turning entries at an angle to fracture or kink zones.

In long-term mine planning and projections, core drilling is the most important method of obtaining data. Drilling data, however, cannot provide a detailed map of roof conditions in advance of mining, but it can and should be used to determine the roof rock type and sequence and its range of variability. Attention to coring the roof and floor should be given. A minimum of 30 feet (9 m) of roof and 10 feet of the floor should be cored in every test hole. Some drill holes should provide cores of the entire bedrock succession to more than 10 feet below the coal to establish correlation of stratigraphic units. The cores should be carefully logged and the data used to compile lithologic thickness and facies maps. In addition, the cores should be sampled to gain geotechnical data, particularly for the purpose of rock-mechanical and mineralogic-petrographic analysis, to supplement the geologic interpretations.

Coal mine planners should attempt to learn as much as possible about earlier mining experience in the area in which they contemplate mining. Knowledge of many previously experienced factors, for instance, roof rock type, faults, and kink zone orientation, can help greatly in laying out a mine to minimize roof problems. Many roof failure patterns occur consistently throughout a mining district. The Illinois State Geological Survey maintains a large quantity of information on geologic conditions in coal mines in Illinois.

Additional recommendations include training underground personnel in basic recognition of geologic features that pose a hazard to roof stability and maintaining a mapping program to record (1) roof lithology, (2) structural geologic features, (3) location and time of roof falls in relation to time of coal removal, (4) bolting type, spacing, and pattern, and (5) location and time of additional roof support. Intensification of underground surveying and systematic sampling of coal and floor and roof rocks for geologic and rock-mechanical testing and analysis is also recommended. Data from exploration drilling and mapping, mine surveys, structural analysis, coal analysis, technical analysis of roof and floor rock, rock-mechanical testing, and roof failures in particular areas may be conveniently stored and retrieved with the aid of a computer as a supplement to existing data files that are open to the public, such as those at the Illinois State Geological Survey.

APPENDIX



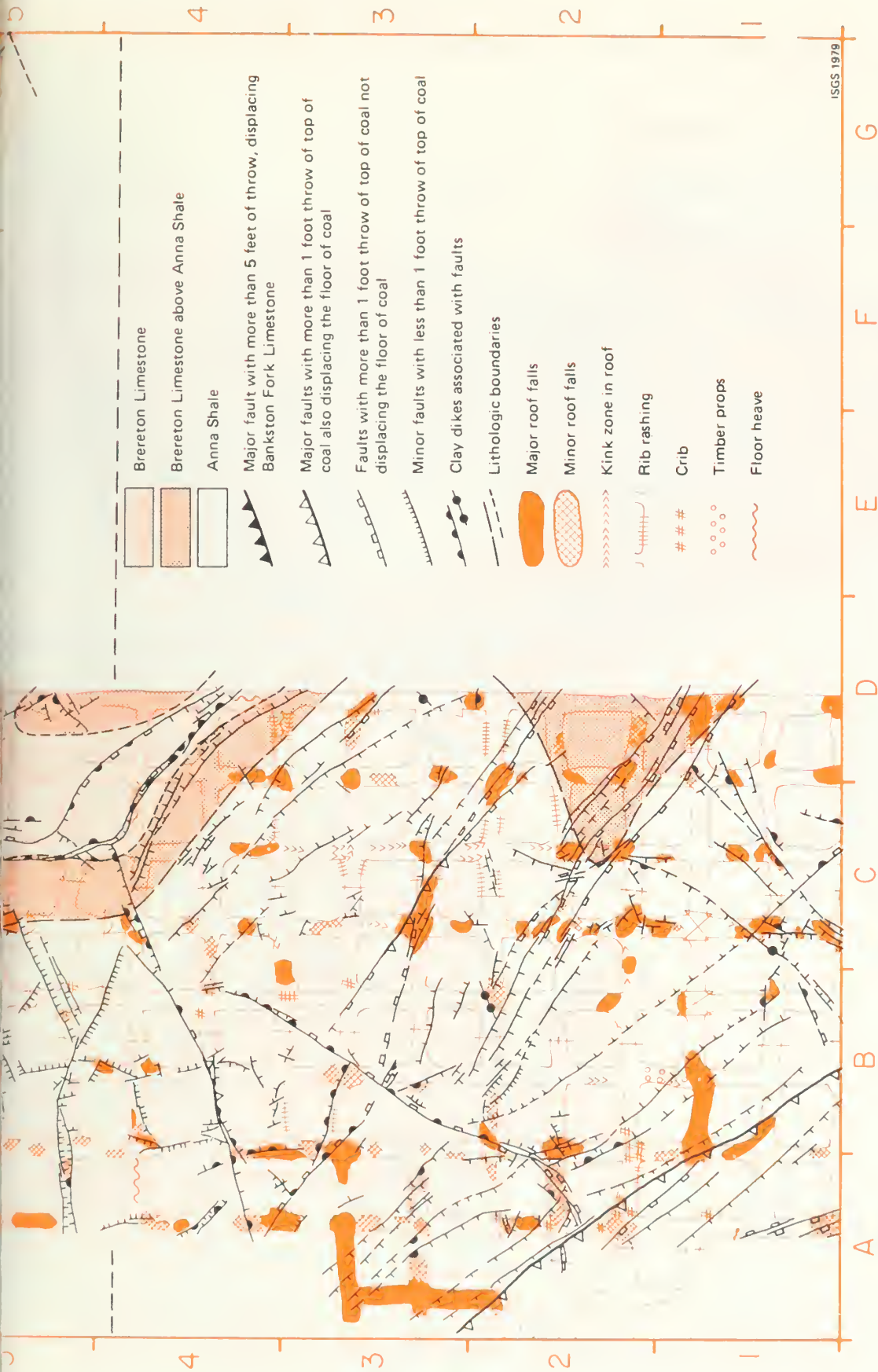


Figure A. Distribution of lithology, of clay-dike faults and clay dikes in the Herrin (No. 6) Coal and its immediate roof strata, and of roof falls and other induced instabilities in study area 1, mine A. (See also fig. 35, p. 32.)

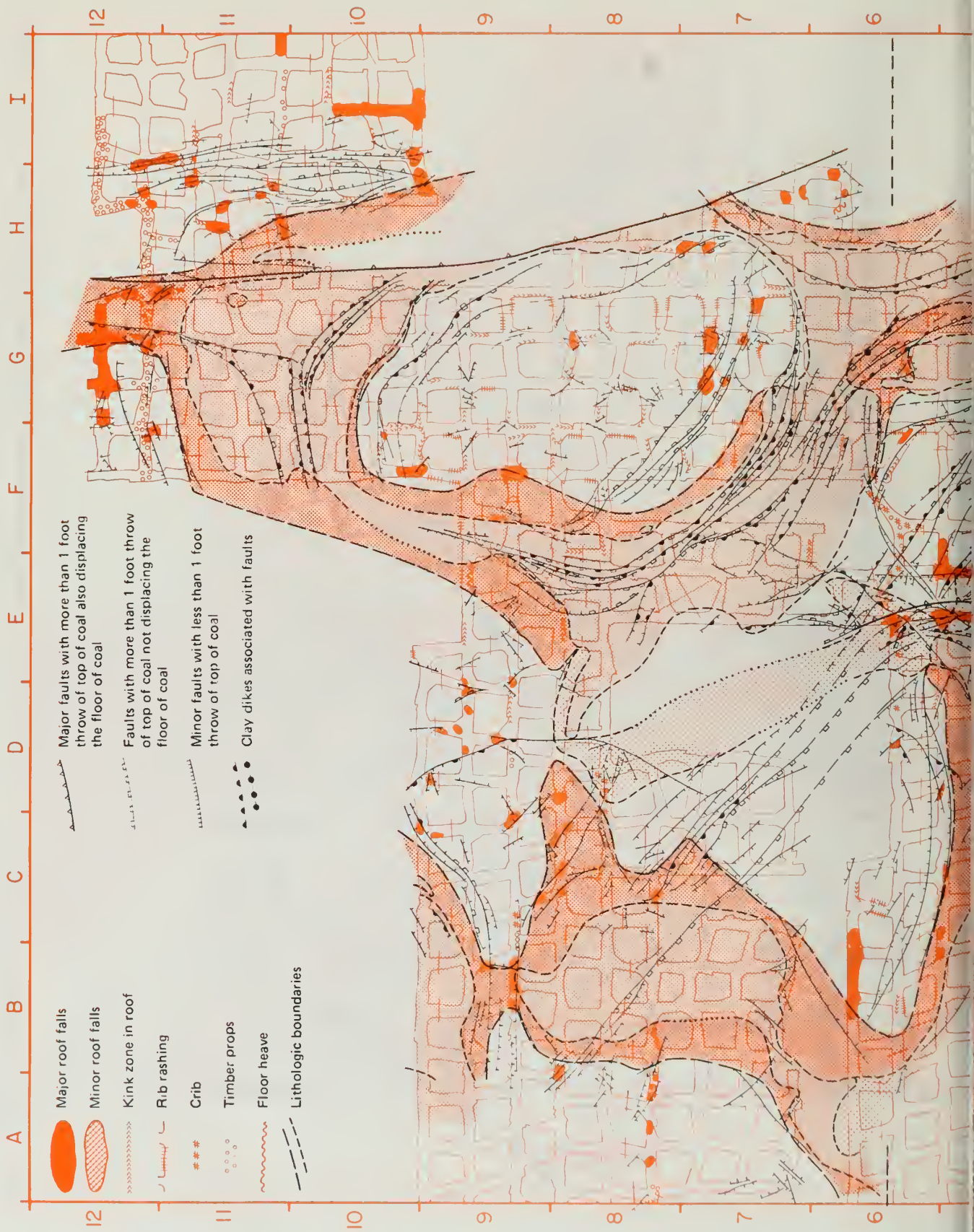
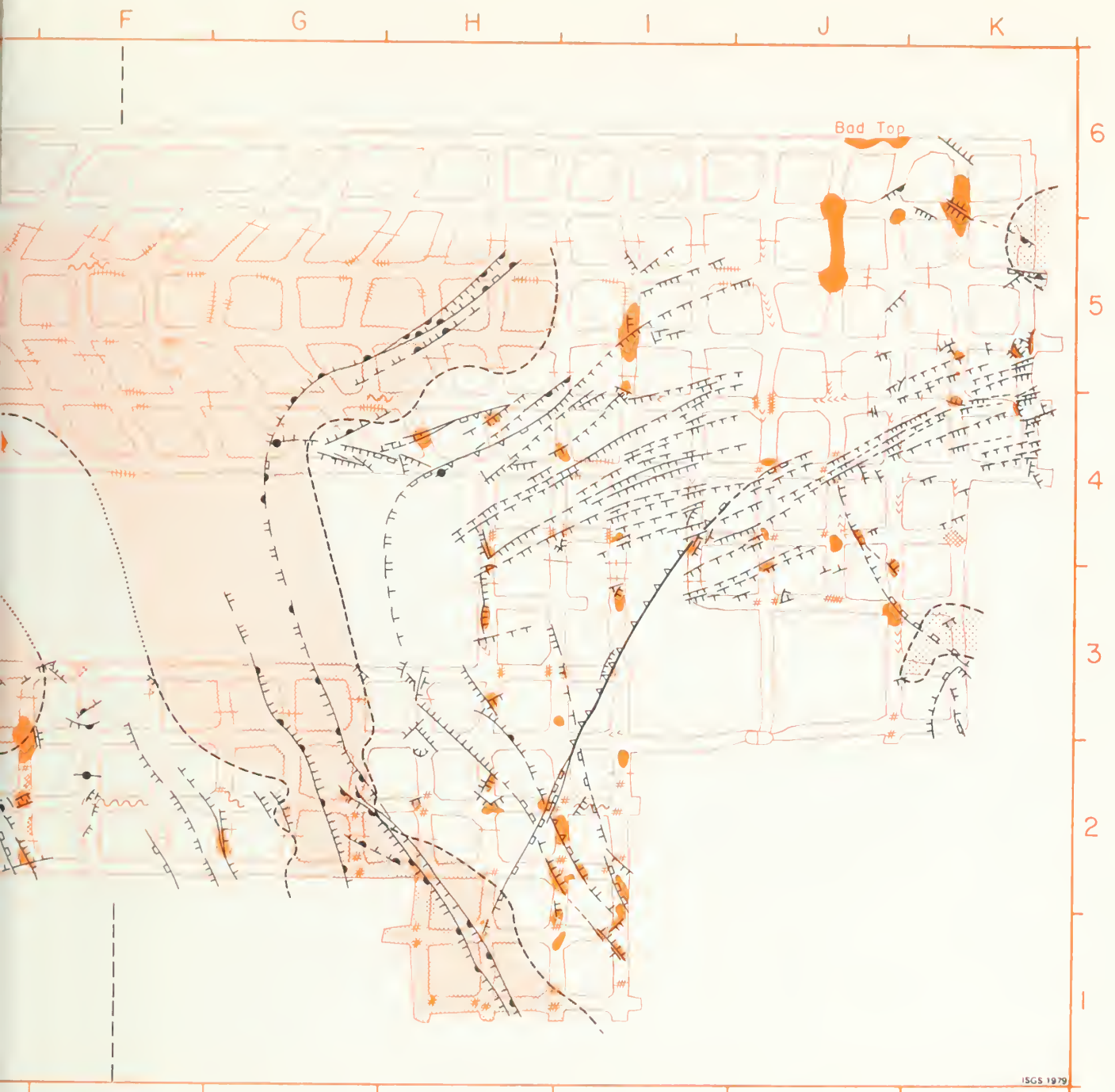




Figure B. Distribution of lithology, of clay-dike faults and clay dikes in the Herrin (No. 6) Coal and its immediate roof strata, and of roof falls and other induced instabilities in study area 2, mine A. (See also fig. 36, p. 33.)

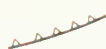
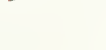


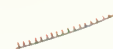


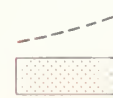


Figure C. Distribution of lithology, of clay-dike faults and clay dikes in the Herrin (No. 6) Coal and its immediate roof strata, and of roof falls and other induced instabilities in study area 3, mine A. (See also fig. 37, p. 34.)



ISGS 1979

-  Major roof falls
-  Minor roof falls
-  Kink zone in roof
-  Rib rashing
-  Crib
-  Floor heave

-  Major faults with more than 1 foot throw of top of coal also displacing the floor of coal
-  Faults with more than 1 foot throw of top of coal not displacing the floor of coal

-  Minor faults with less than 1 foot throw of top of coal
-  Clay dikes associated with faults
-  Lithologic boundaries
-  "Jamestown Coal interval"
-  Brereton Limestone
-  Anna Shale

REFERENCES

- Allgaier, G. J., 1974, Reserves of the Herrin (No. 6) Coal in the Fairfield Basin in southeastern Illinois: unpublished draft, Illinois State Geological Survey.
- Allgaier, G. J., and M. E. Hopkins, 1975, Reserves of the Herrin (No. 6) Coal in southeastern Illinois: Illinois State Geological Survey Circular 489, 31 p.
- Brandow, V. D., H. M. Karara, H. H. Damberger, and H.-F. Krausse, 1976, A nonmetric close-range photogrammetric system for mapping geologic structures in mines: *Photogrammetric Engineering and Remote Sensing*, v. 42, no. 5, p. 637-648.
- Damberger, H. H., 1970, Clastic dikes and related impurities in Herrin (No. 6) and Springfield (No. 5) Coals of the Illinois Basin, in *Depositional environments in parts of the Carbondale Formation—western and northern Illinois*: Illinois State Geological Survey Guidebook 8, p. 111-119.
- Damberger, H. H., 1973, Physical properties of the Illinois Herrin (No. 6) Coal before burial, as inferred from earthquake-induced disturbances: *Compte Rendu, Seventh International Congress of Carboniferous Stratigraphy and Geology*, v. 2, p. 341-350.
- Edwards, M. J., 1976, Analysis of lithologic and structural patterns in the Energy Shale at the Orient #6 Mine, Jefferson County, Illinois: unpublished bachelor's thesis, University of Illinois, Urbana, 32 p.
- Gluskoter, H. G., and M. E. Hopkins, 1970, Distribution of sulfur in Illinois coals, in *Depositional environments in parts of the Carbondale Formation—western and northern Illinois*: Illinois State Geological Survey Guidebook 8, p. 89-95.
- IBM Corporation, 1968, Surface techniques, annotation, and mapping programs for exploration, development, and engineering (STAMPEDE), DOS system 360-370, program number 360D-17.4.001.
- Krausse, H.-F., H. H. Damberger, W. J. Nelson, S. R. Hunt, C. T. Ledvina, C. G. Treworgy, and W. A. White, 1979, Engineering Study of Structural Geologic Features of the Herrin (No. 6) Coal and Associated Rock in Illinois: Volume 1—Summary report. Volume 2—Detailed report. U.S. Department of the Interior, Bureau of Mines, contract H0242017.
- Potter, Paul E., 1957, Breccia and small-scale lower Pennsylvanian overthrusting in southern Illinois: *Bulletin of the American Association of Petroleum Geologists*, v. 41, no. 12, p. 2695-2709.
- Seilacher, A., 1969, Fault-graded beds interpreted as seismites: *Sedimentology*, v. 13, p. 155-159.
- Smith, W. H., and J. B. Stall, 1975, Coal and water resources for coal conversion in Illinois: Illinois State Geological Survey Cooperative Resources Report 4, 79 p.
- Swann, D. H., P. B. DuMontelle, R. F. Mast, and L. H. Van Dyke, 1970, ILLIMAP—A computer-based mapping system for Illinois: Illinois State Geological Survey Circular 451, 24 p.
- Voigt, E., 1962, Frühdiagenetische Deformation der turonen Plänerkalke bei Halle/Westphalen als Folge einer Grossgleitung unter besonderer Berücksichtigung des Phacoid-Problems: *Mitteilungen Geologisches Staatsinstitut Hamburg*, v. 31, p. 146-275.



